

Diversity, distribution, development, and evolution of medullary bundles in Nyctaginaceae

Israel L. da Cunha Neto^{1,7} , Marcelo R. Pace², Norman A. Douglas³, Michael H. Nee⁴, Cyl Farney C. de Sá⁵, Michael J. Moore⁶, and Veronica Angyalossy¹

Manuscript received 10 July 2019; revision accepted 6 February 2020.

¹ Departamento de Botânica, Instituto de Biociências, Universidade de São Paulo, Rua do Matão, 277, Cidade Universitária, CEP 05508-090, São Paulo, SP, Brazil

² Departamento de Botânica, Instituto de Biología, Universidad Nacional Autónoma de México, Ciudad Universitaria, Apartado Postal 70-367, Mexico City, Mexico

³ Department of Biology, University of Florida, P.O. Box 118525, Gainesville, FL 32611 USA

⁴ New York Botanical Garden, 2900 Southern Blvd., Bronx, NY 10458-5126 USA

⁵ Instituto de Pesquisas Jardim Botânico do Rio de Janeiro, Rua Pacheco Leão, 915, Rio de Janeiro, RJ, Brasil

⁶ Department of Biology, Oberlin College, Oberlin, OH 44074 USA

⁷ Author for correspondence (e-mail: israelopescn@gmail.com, israelneto@usp.br)

Citation: da Cunha Neto, I. L., M. R. Pace, N. A. Douglas, M. H. Nee, C. F. C. de Sá, M. J. Moore, and V. Angyalossy. 2020. Diversity, distribution, development, and evolution of medullary bundles in Nyctaginaceae. *American Journal of Botany* 107(5): 1–19.

doi:10.1002/ajb2.1471

PREMISE: Medullary bundles, i.e., vascular units in the pith, have evolved multiple times in vascular plants. However, no study has ever explored their anatomical diversity and evolution within a phylogenetic framework. Here, we investigated the development of the primary vascular system within Nyctaginaceae showing how medullary bundles diversified within the family.

METHODS: Development of 62 species from 25 of the 31 genera of Nyctaginaceae in stem samples was thoroughly studied with light microscopy and micro-computed tomography. Ancestral states were reconstructed using a maximum likelihood approach.

RESULTS: Two subtypes of eusteles were found, the regular eustele, lacking medullary bundles, observed exclusively in representatives of Leucastereae, and the polycyclic eustele, containing medullary bundles, found in all the remaining taxa. Medullary bundles had the same origin and development, but the organization was variable and independent of phyllotaxy. Within the polycyclic eustele, medullary bundles developed first, followed by the formation of a continuous concentric procambium, which forms a ring of vascular bundles enclosing the initially formed medullary bundles. The regular eustele emerged as a synapomorphy of Leucastereae, while the medullary bundles were shown to be a symplesiomorphy for Nyctaginaceae.

CONCLUSIONS: Medullary bundles in Nyctaginaceae developed by a single shared pathway, that involved the departure of vascular traces from lateral organs toward the pith. These medullary bundles were encircled by a continuous concentric procambium that also constituted the polycyclic eustele, which was likely a symplesiomorphy for Nyctaginaceae with one single reversion to the regular eustele.

KEY WORDS Caryophyllales; evo-devo; Nyctaginaceae; ontogeny; primary growth; stem anatomy; trait evolution; vascular bundles.

Medullary bundles are complete vascular bundles located in the pith and may be arranged in two or more concentric rings or as bundles scattered within the pith in addition to the bundles of the stele ring (de Bary, 1884; Esau, 1967; Ogura, 1972; Beck et al., 1982; Schmid, 1982; Mauseth, 1988; Beck, 2010; Isnard et al., 2012). Such organization of the vascular tissue constitutes the “polycyclic eustele” subtype in the stele classification by Beck et al. (1982) and Schmid (1982). Medullary bundles have also been addressed in the context of “anomalous structures” (de Bary, 1884; Eames and MacDaniels, 1925; Metcalfe and Chalk, 1950; Beck, 2010; Yang and Chen, 2017), a concept not followed here, since we consider the so-called anomalous vascular structures to be a variant type of secondary growth (Carlquist, 2001; Angyalossy et al., 2012, 2015). Regardless, medullary bundles are a remarkable feature of vascular plants, which also

contributes to their complexity and morphological diversity (Eames and MacDaniels, 1925; Beck et al., 1982).

Medullary bundles have evolved multiple times in the history of vascular plants, being present in ferns (e.g., Cyatheaceae and Dennstaedtiaceae [*Pteridium*], Ogura, 1927, 1972; Eames and MacDaniels, 1925; Lucansky, 1974), and more frequently in the flowering plants, where they have been recorded in approximately 60 families, including magnoliids (Isnard et al., 2012; Trueba et al., 2015) and eudicots (Wilson, 1924; Lambeth, 1940; Boke, 1941; Holwill, 1950; Metcalfe and Chalk, 1950; Davis, 1961; Esau, 1967; Pant and Bhatnagar, 1975; Raj and Nagar, 1980, 1989; Kirchoff and Fahn, 1984; Mauseth, 1993, 2006; Costea and DeMason, 2001; Schwallier et al., 2017; Kapadane et al., 2019). In some families, this character is found in just a few representatives (e.g., *Nepenthes*,

Nepenthaceae; Schwallier et al., 2017) or is restricted to a specific lineage (subfamily Cactoideae, Cactaceae; Mauseth, 1993, 2006; Terrazas and Arias, 2002), while in others it seems to be widespread within the family (e.g., Amaranthaceae, Nyctaginaceae, Piperaceae) (Metcalfe and Chalk, 1950). However, comparative analyses or investigations within a phylogenetic context are still lacking, except for Cactaceae (Mauseth, 1993, 2006).

Nyctaginaceae is a family distributed in tropical and subtropical regions worldwide, currently encompassing 31 genera and more than 400 species of herbs, subshrubs, lianas, shrubs, and trees (Bittrich and Kühn, 1993; Douglas and Manos, 2007; Douglas and Spellenberg, 2010; Hernández-Ledesma et al., 2015). Medullary bundles are a common feature in Nyctaginaceae, and different studies have aimed to explain their occurrence in relation to the vascularization of the vegetative shoot (Inouye, 1956; Nair and Nair, 1961; Sharma, 1962; Balfour, 1965; Pulawska, 1972; Zamski, 1980). Nevertheless, studies within Nyctaginaceae are restricted to a few genera (i.e., *Boerhavia*, *Bougainvillea*, and *Mirabilis*), and the distribution, anatomy, diversity, and evolution of medullary bundles have yet to be fully characterized.

The structure and ontogeny of medullary bundles for most taxa of Nyctaginaceae remain unknown or need re-evaluation, in part because only the adult stems of these plants have been studied in most cases (de Bary, 1884; Metcalfe and Chalk, 1950) or the anatomical origin and developmental processes have been interpreted differently. For instance, medullary bundles are reported to arise from cauline bundles, those that originate in the shoot apical meristem but do not form leaf traces (Inouye, 1956; Gibson, 1994), or from vascular strands departing from leaves and lateral appendages (Balfour, 1965; Zamski, 1980). There are also cases in which authors failed to recognize the medullary bundles, naming them either “primary bundles” (Nair and Nair, 1961; Stevenson and Popham, 1973; Mikesell and Popham, 1976) or “leaf traces” (Pant and Mehra, 1963; Gibson, 1994). Moreover, while some authors stated that only the innermost bundles are of primary origin (Inouye, 1956), others have argued that at least some of them are of secondary origin (for example, those situated more peripherally; de Bary, 1884; Sabnis, 1921; Balfour, 1965; Pulawska, 1972).

Here, we conducted a detailed anatomical study of the diversity and evolution of the medullary bundles in Nyctaginaceae using a time-calibrated phylogeny as the framework for the analyses. Specifically, we evaluated the occurrence, development, distribution, diversity, and evolution of medullary bundles and how they affect the organization of the eustele in the monophyletic Nyctaginaceae, in which medullary bundles are widespread. This study characterizes for the first time the complexity of the primary vascular system of Nyctaginaceae and shows how different subtypes of eustele have evolved within the family.

MATERIALS AND METHODS

Taxon sampling and material collection

Stems of 62 species representing 25 of the 31 genera of the family Nyctaginaceae were collected either in natural populations, herbaria, or wood collections. Nyctaginaceae is currently subdivided into seven tribes (Douglas and Spellenberg, 2010): Nyctagineae, Pisonieae, Bougainvilleae, Boldoeae, Colignoniae, Leucastereae, and Caribeae. Genera from all tribes were sampled except for the monotypic Caribeae (*Caribea litoralis* Alain), known only from the type collection and which may be extinct (Douglas and Spellenberg, 2010). The sampled species, habits, number of specimens studied, and the type

of anatomical analysis performed for each species are summarized in Table 1. At least one species from the main lineages of Nyctaginaceae was selected for the developmental study (Table 1). For these species, we sampled stems from the shoot apex until the fifth internode. In addition, fully developed stems were also analyzed. For that, different samples along the stem and at the base of the plant were obtained in the case of herbs, subshrubs, shrubs, scandent shrubs, and lianas, while branches up to 1.5–2 cm in diameter were analyzed for trees. Detailed information on the species, localities of collection, and herbaria where vouchers were deposited is included in Appendix 1.

Besides Nyctaginaceae, 11 species as outgroups for the ancestral character state reconstruction were sampled (further information below). The species were distributed across Agdestidaceae, Petiveriaceae, and Phytolaccaceae, which represent three of the four most closely related families to Nyctaginaceae within the phytolaccoid clade (sensu Walker et al., 2018). No information could be obtained for Sarcobataceae, the remaining family in the phytolaccoid clade. For these 11 species, character state information was obtained either from natural populations, wood or herbarium collections or directly from original published images (see Appendix 1 for information).

Anatomical procedures

For anatomical studies, all specimens collected in the field were immediately fixed in either FAA (formaldehyde–acetic acid–70% ethanol, 1:1:18 v/v) (Berlyn and Miksche, 1976) or 70% isopropyl alcohol for a week, and then stored in 70% ethanol (Johansen, 1940). Subsequently, samples from different developmental stages were either dehydrated in an ethanol series and embedded in a methacrylate resin (Historesin; Leica Microsystems, Heidelberg, Germany), or dehydrated in a butanol series, infiltrated with mixtures of butanol + Paraplast with increasing concentrations of paraplast and embedded in paraplast (Fisher Healthcare, Houston, TX, USA) (Johansen, 1940). Transverse and longitudinal sections were cut using either a rotary (Leica RM2145, Nussloch, Eisfeld, Germany) or a sliding microtome (Leica SM2010R). Sections cut from methacrylate were 5–8 μm thick and stained with 0.05% w/v toluidine blue O in 0.1 M phosphate buffer (pH 4.7; O'Brien et al., 1964), while sections cut from Paraplast were 10–12 μm thick and doubled-stained in aqueous 1% w/v astra-blue and 1% w/v safranin (Bukatsch, 1972). Samples from herbaria and/or wood collections were rehydrated by boiling the material in a mixture of water and glycerin (Angyalossy et al., 2016). Afterward, small samples were embedded in methacrylate resin and stained with 0.05% toluidine blue. For even larger stem samples, inclusion in polyethylene glycol 1500 was adopted (Barbosa et al., 2010). Permanent steel knives perfectly sharpened with sandpaper were used (Barbosa et al., 2018). The slides were mounted in synthetic resin (Permount; Fisher Scientific, Fair Lawn, NJ, USA). In addition, some samples were dehydrated in ethanol, hand-sectioned, doubled-stained in 1% astra-blue and 1% safranin and mounted in 50% v/v glycerin.

For examining the morphology of vessel elements and fibers, tissue was macerated using Jeffrey's solution (aqueous 10% nitric acid + 10% chromic acid v/v; Johansen, 1940). The dissociated material was washed in water, stained with safranin, and the slides were mounted in 50% glycerin.

The anatomical analyses and photographs were performed using a Leica DMBL light microscope coupled with a digital camera (Leica DFC310, Leica Microsystems, Wetzlar, Germany). The images were edited and, sometimes, auto-aligned to build larger pictures

TABLE 1. Species name for all studied Nyctaginaceae and outgroups, including habit, number of specimens analyzed, and type of anatomical analysis (a, development; b, primary growth; c, secondary growth; d, maceration). Species with development studied (“a”) are in bold. For information on collection site and vouchers, see Appendix 1.

Taxon	Habit	No. of specimens analyzed	Anatomical analysis
Nyctagineae			
<i>Abronia fragrans</i>	Herb	1	b-c
<i>Abronia nealleyi</i>	Herb	1	a-d
<i>Acleisanthes acutifolia</i>	Herb	1	c
<i>Acleisanthes chenopodioides</i>	Herb	3	a-d
<i>Acleisanthes lanceolata</i>	Herb	2	b-c
<i>Acleisanthes longiflora</i>	Subshrub	1	b-c
<i>Allionia choisyi</i>	Herb	1	c
<i>Allionia incarnata</i>	Herb	5	a-d
<i>Anulocaulis leiosolenus</i> var. <i>leiosolenus</i>	Herb	3	a-d
<i>Anulocaulis leiosolenus</i> var. <i>gypsogenus</i>	Herb	3	c
<i>Boerhavia diffusa</i>	Subshrub	2	c
<i>Boerhavia hereroensis</i>	Herb	1	b-c
<i>Boerhavia linearifolia</i>	Herb	2	b-c
<i>Boerhavia torreyana</i>	Herb	2	b-c
<i>Boerhavia wrightii</i>	Herb	2	c
<i>Commicarpus scandens</i>	Scandent-shrub	3	a-d
<i>Cyphomeris gypsophilooides</i>	Herb	2	a-d
<i>Mirabilis aggregata</i>	Herb	1	b-c
<i>Mirabilis</i> cf. <i>albida</i>	Herb	2	a-d
<i>Mirabilis jalapa</i>	Subshrub	1	a-d
<i>Mirabilis viscosa</i>	Herb	1	c
<i>Mirabilis</i> sp.	Herb	1	c
<i>Nyctaginia capitata</i>	Herb	2	a-d
<i>Okenia hypogea</i>	Herb	3	a-d
Pisonieae			
<i>Grajalesia fasciculata</i>	Tree	2	a-c
<i>Guapira linearibracteata</i>	Tree	1	c
<i>Guapira pernambucensis</i>	Scandent-shrub	2	a-c
<i>Guapira graciliflora</i>	Tree	1	a-c
<i>Guapira laxa</i>	Tree	1	a-d
<i>Guapira ligustrifolia</i>	Tree	1	c
<i>Guapira opposita</i>	Tree	1	c
<i>Neea delicatula</i>	Tree	1	c
<i>Neea hermaphrodita</i>	Tree	2	a-c
<i>Neea laetevirens</i> Standl.	Tree	1	c
<i>Neea macrophylla</i>	Tree	1	c
<i>Neea ovalifolia</i>	Tree	1	c
<i>Neea psychotrioides</i>	Tree	1	c
<i>Pisonia aculeata</i>	Liana	2	a-d
<i>Pisonia zapallo</i>	Tree	1	c
<i>Pisonia</i> sp1.	Tree	1	c
<i>Pisonia</i> sp2.	Tree	1	a-c
<i>Pisonia</i> sp3.	Tree	1	c
<i>Pisoniella arborescens</i>	Liana	2	a-c
<i>Pisoniella glabrata</i>	Liana	2	a-d
Bougainvilleae			
<i>Belemia fucsioides</i>	Liana	2	c
<i>Bougainvillea berberidifolia</i>	Shrub	2	a-d
<i>Bougainvillea campanulata</i>	Shrub	2	a-c
<i>Bougainvillea modesta</i>	Tree	2	c
<i>Bougainvillea stipitata</i>	Tree	2	b-c
<i>Bougainvillea spectabilis</i>	Scandent-shrub	1	c
<i>Bougainvillea</i> sp1.	Shrub	1	c

(Continued)

TABLE 1. (Continued)

Taxon	Habit	No. of specimens analyzed	Anatomical analysis
<i>Bougainvillea</i> sp2.	Shrub	1	c
<i>Phaeoptilum spinosum</i>	Shrub	1	c
Colignonieae			
<i>Colignonia glomerata</i>	Liana	2	a-d
<i>Colignonia rufopilosa</i>	Liana	1	c
Boldoeae			
<i>Cryptocarpus pyriformis</i>	Liana	1	c
<i>Salpianthus arenarius</i>	Shrub	1	c
<i>Salpianthus macrodontus</i>	Shrub	1	c
<i>Salpianthus purpurascens</i>	Shrub	1	a-d
Leucastereae			
<i>Andradea floribunda</i>	Tree	2	a-c
<i>Leucaster caniflorus</i>	Liana	3	a-c
<i>Ramisia brasiliensis</i>	Tree	2	a-c
<i>Reichenbachia hirsuta</i>	Shrub	2	a-d
Outgroups*			
Agdestidaceae			
<i>Agdestis clematidea</i>	Liana	1	—
Petiveriaceae			
<i>Gallesia integrifolia</i>	Tree	2	a-c
<i>Hillieria latifolia</i>	Herb	1	—
<i>Monococcus echinophorus</i>	Shrub	1	—
<i>Petiveria alliacea</i>	Herb	2	—
<i>Trichostigma octandrum</i>	Liana	1	—
<i>Rivina humilis</i>	Herb	2	—
<i>Seguiera americana</i>	Tree	2	—
<i>Seguiera langsdorffii</i>	Shrub	1	—
Phytolaccaceae			
<i>Phytolacca dioica</i>	Tree	2	—

Note: Based mostly on the literature, except for *Gallesia integrifolia*, *Seguiera americana* and *Seguiera langsdorffii*. See Appendix 1 for details.

using Photoshop (v. CS5, 64-bit; Adobe, San Jose, CA, USA) or Leica Application Suite (LAS, v. 4.0).

Micro-computed tomography

A fixed sample of *Colignonia glomerata* (less than 2 mm thick) was used for micro-computed tomography (SkyScan 1176, Bruker, Kotich, Belgium). The scanner was adjusted with a 50 kV/500 µA power supply, Al 0.5 mm filter, and 18 µm average resolution. After three-dimensional reconstruction, images were captured using CTvox 3D visualization software (v. 3.1.2 64-bit; Micro Photonics, Allentown, PA, USA). The micro-CT analyses allowed the observation of the stem structure sequentially and nondestructively. The results obtained with this technique were compared with anatomical sections.

Phylogeny and ancestral character state reconstruction

A well-supported genus-level molecular phylogeny of Nyctaginaceae (Douglas and Manos, 2007; Douglas and Spellenberg, 2010) was used as the basis for ancestral character state reconstruction for the different eustele subtypes. Since some species sampled in this study were not sampled in that phylogeny, the tree was edited to include only the species sampled in this work by collapsing them into the least inclusive nodes. After the species that were not sampled in our anatomical analyses were pruned, a tree containing all the taxa analyzed in the

present study was obtained, and this tree was used for ancestral character state reconstructions. To establish the relationship within tribe Pisonieae, we followed the most recent classifications by Rossetto et al. (2019). A tree including representatives of four sister lineages (i.e., Petiveriaceae, Phytolaccaceae, Sarcobataceae, and Agdestidaceae) was also used to perform reconstruction analyses. For this tree, the relationships established by Walker et al. (2018) were followed. Among these families, Agdestidaceae were monotypic, Sarcobataceae are monogeneric (ca. two species), while Phytolaccaceae have three genera, and Petiveriaceae have nine genera (Stevens, 2001 onward; Hernández-Ledesma et al., 2015).

The ancestral character reconstruction analyses were performed using maximum likelihood algorithms as implemented in Mesquite (ver. 3.6; Maddison and Maddison, 2009).

RESULTS

Primary vascular system: eustele subtypes

In Nyctaginaceae, two subtypes of eustele were observed, the regular eustele (Fig. 1A, B) and the polycyclic eustele (Fig. 1C, D). The

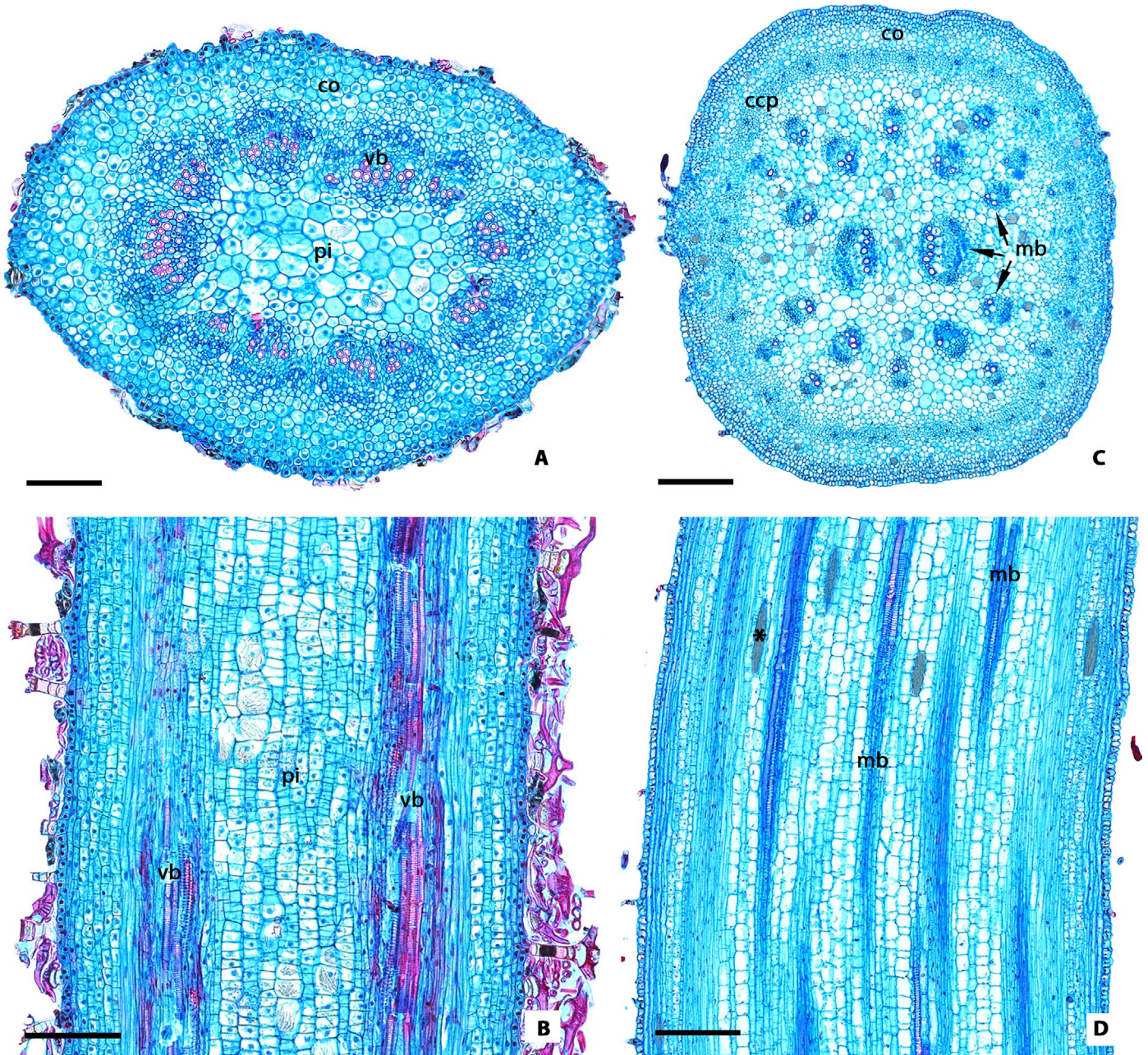


FIGURE 1. Subtypes of eustele in Nyctaginaceae. (A, B) *Reichenbachia hirsuta*, regular eustele, formed by collateral vascular bundles forming a ring that delimits the pith. (C, D) *Pisoniella glabrata*, polycyclic eustele, formed by medullary bundles arranged in rings inside the pith and encircled by a continuous concentric procambium. Asterisk, raphides; co, cortex; ccp, continuous concentric procambium; mb, medullary bundle; pi, pith; vb, vascular bundle. Scale bars: A = 100 μ m; B = 150 μ m; C, D = 200 μ m. Stained with astra blue and safranin.

regular eustele was characterized by the presence of a discrete ring of collateral bundles delimiting the pith (Fig. 1A), whereas the polycyclic eustele was marked by several medullary bundles within the pith and encircled by a continuous concentric procambium that later differentiated into vascular bundles (Fig. 1C). In the following sections, we described the different developmental, structural, and evolutionary aspects of medullary bundles within Nyctaginaceae.

Origin and development of medullary bundles

In Nyctaginaceae, medullary bundles originated from procambial strands that interconnected the stem with lateral organs or appendages, including leaves, branches, and thorns (Figs. 2A–E, 4A–D, 5A). The medullary bundles were the first vascular tissues formed in the polycyclic eustele (Figs. 2A–E, 4C, D), followed by a new, continuous procambial layer that subsequently resulted in vascular bundles (see below *Continuous concentric procambium*). As stem development progressed, additional leaf, bud, and/or thorn traces contributed to the appearance of new medullary bundles externally to the ones that had already established, as seen in *Colignonia glomerata* when comparing early- and later-formed nodes and internodes (Fig. 2A). The same was observed in *Bougainvillea berberidifolia* (Fig. 5A–C).

At the nodal level, medullary bundles sometimes twisted, underwent anastomoses and/or bifurcations, which eventually resulted in changes in their arrangement, size, and disposition (Figs. 2A, 3A–B, 5A–C). In *C. glomerata*, numerous anastomoses were observed, forming what is known as a nodal plexus (Fig. 2A). As new leaf, thorn, and bud traces were produced, some of them anastomosed with already present medullary bundles (Fig. 5A–C), so that their number did not increase indefinitely.

Organization and diversity of medullary bundles

During primary growth, at the first internode near the shoot apex, different organizations of medullary bundles were observed in different taxa (Fig. 6A–I). The number of medullary bundles in Nyctaginaceae varied from eight to more than 20, as seen in *Pisoniella glabrata* (Fig. 1C) and *C. glomerata* (Fig. 6F). The vascular bundles showed three general types (Table 2). Type 1 consisted of eight medullary bundles distributed in a pair of three opposite bundles and two larger ones either in the center (Fig. 6A, C) or forming a ring (Fig. 6B, D–E). Type 2 consisted of ≥ 10 medullary bundles regularly spaced, arranged in two to three concentric rings; the inner ring is composed of larger bundles, and the outer one constituted of smaller bundles (Figs. 1C, 6F). Type 3 consisted of ≥ 10 medullary bundles in a nonspecific arrangement (Fig. 6G–I). Species with eight medullary bundles represented the most common pattern (type 1), although small variations in number and arrangement occurred in each type. The organization of medullary bundles was independent from phyllotaxy and the presence or absence of thorns (Table 2). For example, different genera in tribe Nyctagineae such as *Abronia*, *Acleisanthes*, *Boerhavia*, and *Nyctaginia* had the same phyllotaxy (i.e., opposite), but different types of medullary bundles were found among them (Table 2).

The ancestral character state reconstruction (Fig. 12) suggested type 3 as the most likely ancestral character state for the ancestor of all Nyctaginaceae (45% likelihood presence versus 12.5% for type 1, 22.5% for type 2, and 20% for medullary bundles

absent). Types 1 and 2 had multiple, parallel evolutions within the family, being present in taxa with different habits and from different tribes. There was no single character state that defined an entire clade.

In some species, the number and arrangement of medullary bundles were found to be constant throughout the species life span, such as in the two species of *Pisoniella* (Fig. 6E) and some species of *Neea* and *Guapira*. *Pisoniella arborescens* typically belonged to type 1, but also showed one sample with 10 medullary bundles organized in the same arrangement. In other taxa, the number and arrangement of medullary bundles in stems with secondary growth showed frequent variations derived from anastomoses and/or bifurcations at the nodal regions (Figs. 2A, 5A–C).

Anatomy of medullary bundles

In all taxa studied, the medullary bundles were constituted of phloem to the outside and xylem to the inside, thus being collateral (Fig. 7A, B). During primary growth, medullary bundles were composed solely of conducting cells and parenchyma (Fig. 8B, C). Vessel elements in the primary xylem had different types of wall thickening, varying between annular and helical (Fig. 8B, C).

In all species, as stem secondary growth begun, the medullary bundles also underwent secondary growth (Fig. 8D–G). The secondary xylem was marked by the presence of pitted vessels, fibers, and sometimes rays (Fig. 8D–G). In mature stems, medullary bundles were maintained, showing vessels with the different types of wall thickenings, varying between annular to pitted (Fig. 8E). As the secondary growth proceeded, cells from the primary phloem were crushed to a greater or lesser extent, forming a variable amount of nonconducting, sometimes collapsed phloem (Fig. 8D). On the other hand, even medullary bundles on fully developed stems had conducting xylem and phloem, which in some cases showed little crushed phloem, but several living sieve-tube elements, recognized by the presence of protoplasts in their companion cells (Fig. 8G).

In *Cryptocarpus pyriformis* and some species within tribe Pisonieae (e.g., *Guapira ligustrifolia*, *Neea ovalifolia*), fibers encircling the phloem and to some extent the xylem were observed, as evident in *G. ligustrifolia* (Fig. 9A). In adult stems of *Phaeoptilum spinosum*, the medullary bundles were surrounded by lignified pith tissue (Fig. 9B). In most species, numerous parenchymatic cells containing starch grains were observed in the pith and/or around the medullary bundles, as seen in *Acleisanthes chenopodioides* (Fig. 9C).

Continuous concentric procambium

In addition to the medullary bundles, the primary vascular system in Nyctaginaceae species with polycyclic eustele had an additional developmental step, with the formation of a hollow continuous concentric procambium (Figs. 1C, 2A, 10A–F). This continuous concentric procambium appeared early in stem development, after the second or third node (Figs. 2A, 10A), immediately after the establishment of the medullary bundles (Figs. 2E, 4D, 10A–D). It was characterized by cells with dense cytoplasm, round or irregular contour, and smaller size, as seen in cross section (Fig. 10C, D). These same cells were elongated or appeared fusiform in longitudinal sections (Fig. 10E, F). Later, these procambial cells underwent several periclinal and anticlinal divisions in some regions (Fig. 10D), resulting in the differentiation of primary xylem and phloem in discrete collateral bundles (Fig. 10A–C),

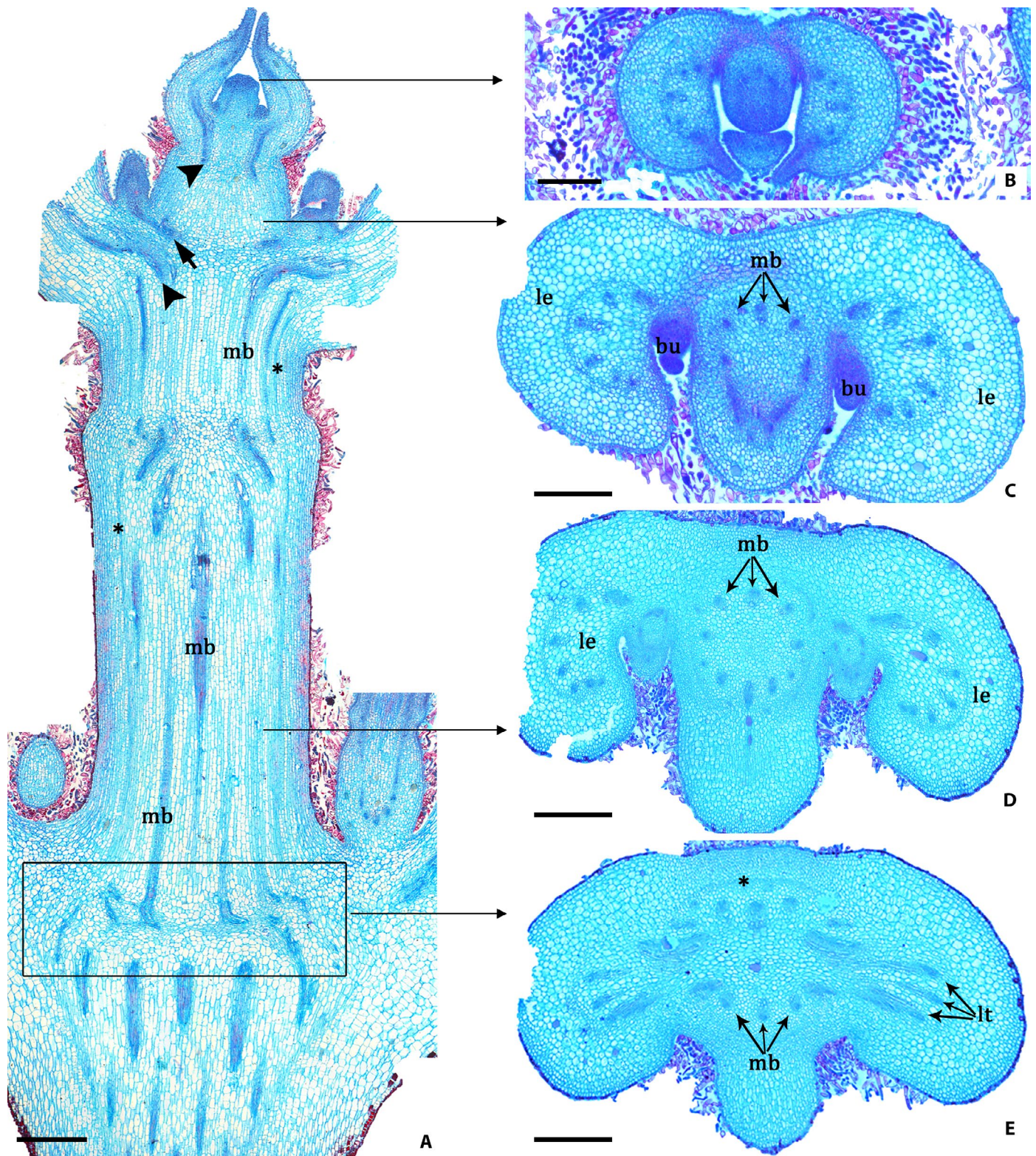


FIGURE 2. Origin and development of medullary bundles in *Colignonia glomerata*. (A) Shoot apex with leaf (arrowheads) and bud (arrow) traces in which medullary bundles anastomose and/or bifurcate. (B–E) Sequence of images from the apex toward developed internodes showing establishment of medullary bundles. Horizontal arrows indicate approximate levels of cross sections. (B) Shoot apical meristem without differentiated medullary bundles. (C–E) Developed medullary bundles in the stem. Notice nodal region in (E) showing three medullary bundles functioning as leaf traces. Asterisk, continuous concentric procambium; bu, axillary bud; mb, medullary bundles; le, leaf; lt, leaf trace. Scale bars: A, C–E = 400 μ m; B = 200 μ m. Stained with astra blue and safranin.

and a ring of parenchymatic cells in the outermost part of the vascular cylinder (Fig. 10E, F). As a result, several vascular bundles had differentiated along the circumference of the continuous concentric procambium establishing a single ring outside the medullary bundles and internally to the starch sheath (Fig. 10A, B).

Unlike the species with polycyclic eusteles, the representatives of tribe Leucastereae had the primary vascular system formed solely by a ring of collateral vascular bundles (Fig. 1A). In these species, the development of the vascular bundles followed a regular pattern in which the vascular bundles delimited the pith, i.e., forming a typical eustele (Fig. 1A).

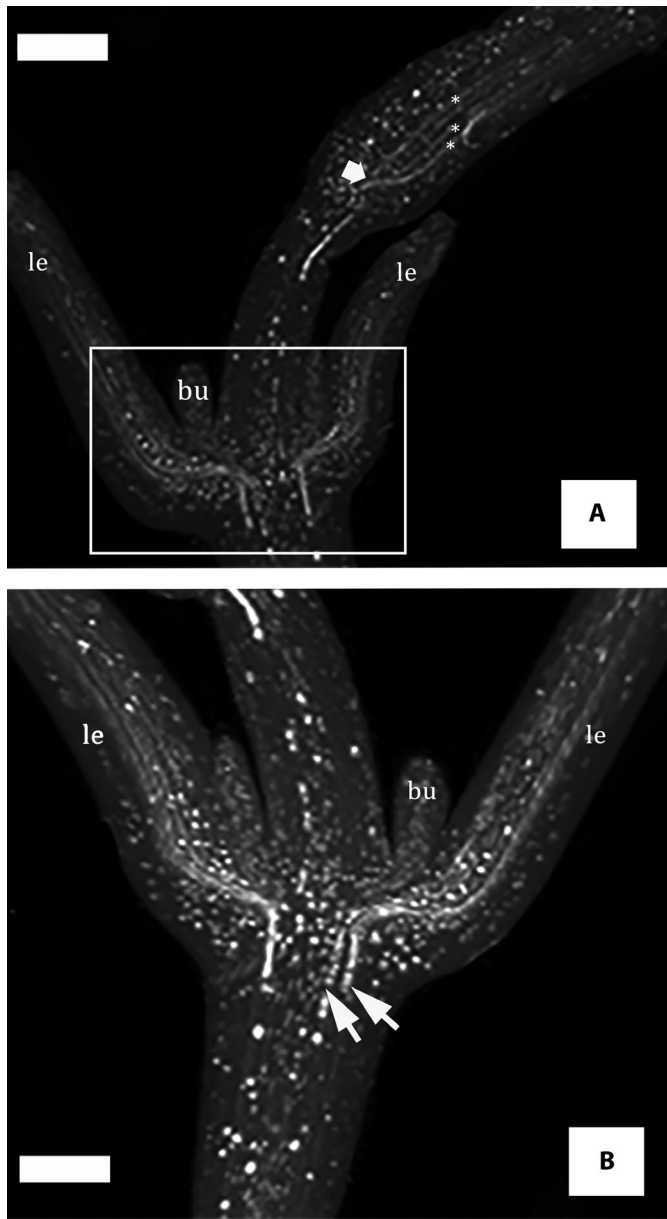


FIGURE 3. Micro-computed tomography images of *Colignonia glomerata*. (A) General view of stem showing trajectory of medullary bundles (asterisks), which anastomose at the nodal region (thick arrow). (B) Close-up of boxed area A in the mirror side, indicating bifurcation of procambial strands (arrows), which establishes as medullary bundles in the pith. bu, axillary bud; le, leaf. Scale bars: 2000 μ m.

Ancestral state reconstruction of the eustele subtypes onto the phylogeny of Nyctaginaceae is shown in Fig. 12. Ancestral character state reconstruction of eustele subtypes across Nyctaginaceae suggested that the ancestral state for the family was the polycyclic eustele (78% presence; 22% absence), with one independent loss to the regular eustele in tribe Leucastereae.

Among the outgroups, we found that most representatives of Petiveriaceae had a regular eustele (i.e., *Gallesia*, *Hillieria*, *Monococcus*, *Petiveria*, *Trichostigma*, *Rivina*, and *Seguieria*); no information was obtained for the remaining genera (i.e., *Ledenbergia* and *Schindleria*). In contrast, the representatives of other outgroup families were found to have the polycyclic eustele, as in *Agdestis clematidea* (Agdestidaceae) and *Phytolacca dioica* (Phytolaccaceae). The analysis including Nyctaginaceae and the representatives of the sister families indicate that the ancestor of the phytolaccoid clade also had medullary bundles (81% presence; 19% absence), with one independent loss in the ancestors of Petiveriaceae and Nyctaginaceae (tribe Leucastereae) (Fig. 12). Therefore, the presence of medullary bundles was most likely a symplesiomorphy for Nyctaginaceae.

DISCUSSION

The evolution of different stele types (and subtypes) is one of the crucial aspects in the diversification of vascular plants (Eames and MacDaniels, 1925; Esau, 1954; Beck et al., 1982). However, the vascular architecture in plants with medullary bundles has long been considered difficult to characterize (Wilson, 1924; Davis, 1961), which makes this topic either controversial or little understood in several aspects, from terminology—with the use of different names (see Nair and Nair, 1961; Schmid, 1982; Gibson, 1994)—to its potential adaptive and/or evolutionary significance. In a general sense, additional vascular tissues in roots and stems, have been thought to be adaptations for higher capacity in the storage and translocation of water and photosynthates, being advantageous especially for some plants occurring in harsh environments (Holwill, 1950; Mauseth, 1993; Carlquist, 2001; Hearn, 2009; Ogburn and Edwards, 2013; Males, 2017). However, the functional significance of medullary bundles is still unclear, and explicit physiological studies are needed to address this question.

Origin of medullary bundles and the continuous concentric procambium

Various reports have explored the origin of medullary bundles. Some suggested that the medullary system originates from independent procambial strands in the shoot apical meristem or as cauline bundles (e.g., Apiaceae: Lambeth, 1940; Cactaceae: Boke, 1941; de Bary, 1884; Nyctaginaceae: Inouye, 1956), while others suggested an origin from regular stelar bundles that branch toward the pith (e.g., Melianthaceae: Metcalfe and Chalk, 1950; Phytolaccaceae: Kirchoff and Fahn, 1984), from the rib meristem (e.g., Cactaceae: Boke, 1941; Convolvulaceae: Pant and Bhatnagar, 1975) or even from mature parenchyma pith cells (e.g., Cactaceae: MacDougal, 1926; Cyatheaceae [ferns]: Lucansky, 1974; Convolvulaceae: Kapadane et al., 2019). In addition, medullary bundles are believed to arise by conversion of intraxylary phloem as for the Cucurbitaceae (Worsdell, 1915), Apocynaceae and Gentianaceae (Metcalfe and Chalk, 1950), and Euphorbiaceae (Hayden and Hayden, 1994). Our findings for Nyctaginaceae did not support any of these statements. The origin of medullary bundles in Nyctaginaceae conforms with the generalization that they arise from

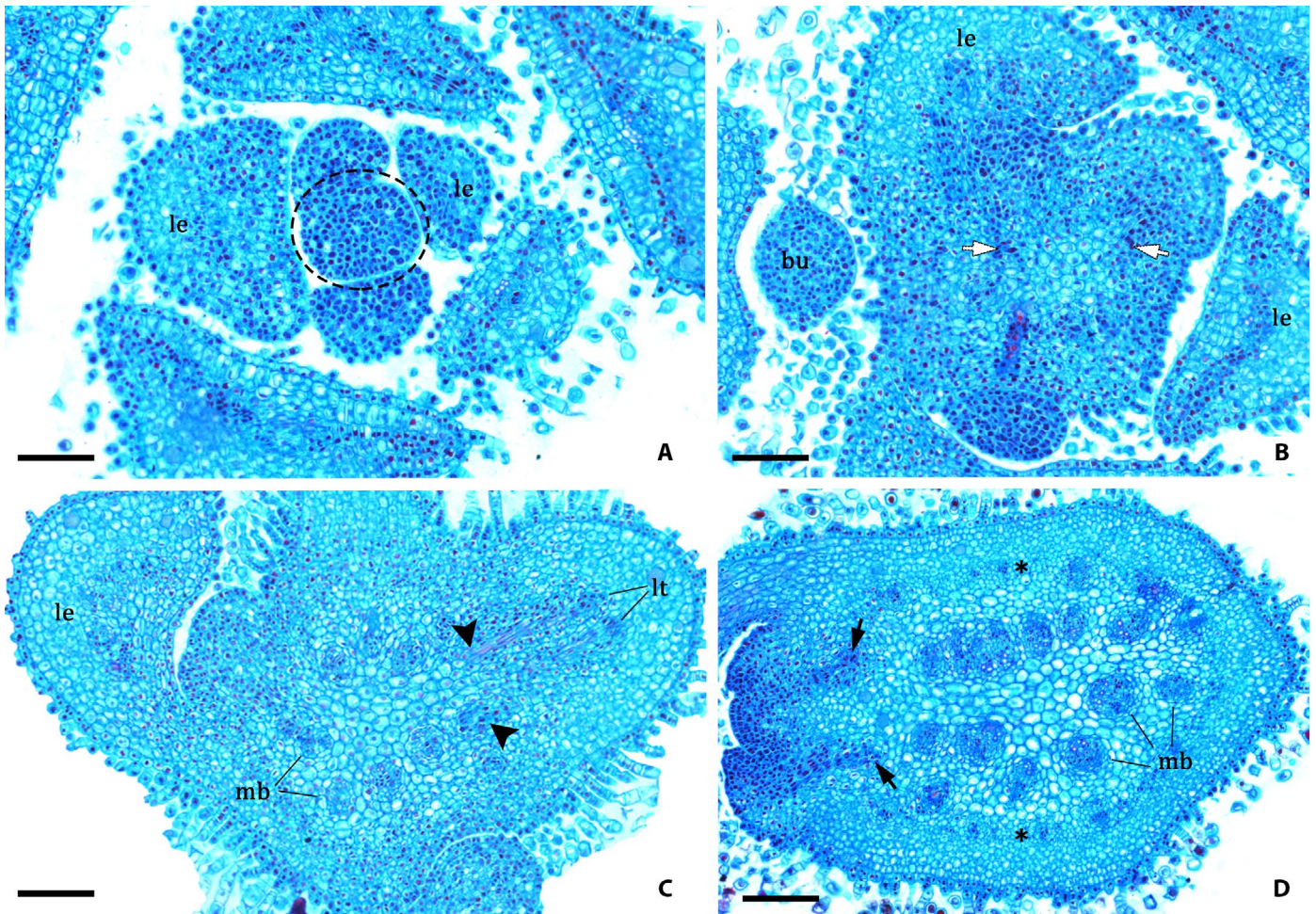


FIGURE 4. Origin and development of medullary bundles in *Bougainvillea berberidifolia*. (A–D) Sequence of images from apex toward more developed internodes showing establishment of medullary bundles from leaves and buds. (A) Shoot apical meristem without differentiated medullary bundles (dashed line). (B) Differentiation of procambial cells (dark stained) from developing leaf traces (white arrows). (C) Differentiated medullary bundles and two future medullary bundles (arrowheads) arising from leaf traces. (D) Greater number of medullary bundles and two new medullary bundles arising from axillary bud (black arrows). Notice the developing continuous concentric procambium (asterisks). bu, axillary bud; le, leaf; lt, leaf trace; mb, medullary bundle. Scale bars: 100 μm . Stained with astra blue and safranin.

procambial traces associated with leaves, buds, thorns, and inflorescences (Nair and Nair, 1961; Sharma, 1962; Stevenson and Popham, 1973; Mikesell and Popham, 1976; Zamski, 1980).

As pointed out by other authors (de Bary, 1884; Inouye, 1956; Pant and Mehra, 1961, 1963) and observed in the present study, medullary bundles may eventually anastomose or bifurcate in the nodes on their trajectory between the lateral organs and the axis. In our study, this pattern was particularly evident in *Colignonia glomerata*, with the formation of a nodal plexus, comparable to those described for monocot stems (Tomlinson and Fisher, 2000; Vita et al., 2019). Similarly, instead of “ending blindly in the stem” as mentioned by earlier authors (Lambeth, 1940; Pant and Bhatnagar, 1975), medullary bundles eventually shifted their trajectory and/or anastomosed with other bundles. Given that one or more bundles frequently connect among them, forming a single bundle, phenomena such as shifting anastomoses or bifurcations of medullary bundles directly interfere in their organization in stem cross sections. Similar phenomena have also been reported for Amaranthaceae and Convolvulaceae, among other families (Wilson, 1924; Pant and

Mehra, 1961, 1963; Pant and Bhatnagar, 1975) (further explored later in *Arrangement of medullary bundles and their independence from shoot morphology*).

Our observation and description of the continuous concentric procambium is fundamental for understanding the primary vascular system in Nyctaginaceae. Three main aspects need to be highlighted regarding the presence of the continuous concentric procambium: (1) it occurs in all species with medullary bundles; (2) as a primary meristem, it produces primary tissues organized in vascular bundles; (3) they constitute part of the primary vascular system; i.e., they are part of the polycyclic eustele.

Previous authors have generally overlooked or given different denominations for this external continuous concentric procambium (de Bary, 1884; Pant and Mehra, 1961, 1963; Balfour and Philipson, 1962; Sharma, 1962; Balfour, 1965; Zamski, 1980). As a result, different terms have been used to name this meristem and its products, including perimedullary bundles and outer ring (Zamski, 1980), third ring (Inouye, 1956), peripheral or “belated” ring (Pant and Mehra, 1961, 1963), peripheral procambial ring (Sharma,

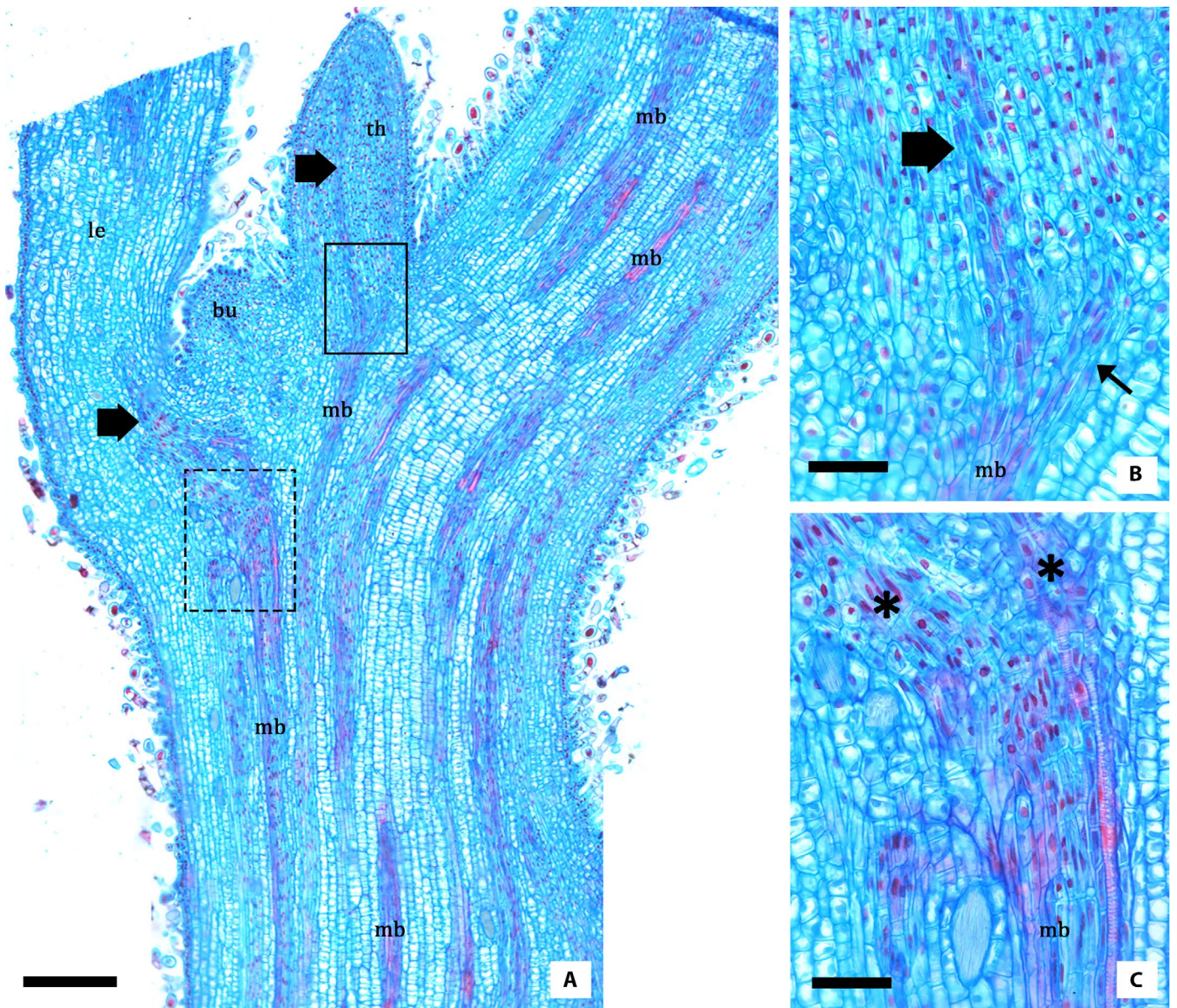


FIGURE 5. Details of the development of medullary bundles in *Bougainvillea berberidifolia*. (A) Overview of stem internodes showing the trajectory of medullary bundles. Notice leaf and thorn traces (thick arrows) which will anastomose with previous established medullary bundles. Box and dashed box indicate close-up in figures (B) and (C), respectively. (B) Detail of thorn trace (thick arrow) diverging towards the pith and fusing with another medullary bundle (thin arrow). (C) Detail of leaf traces (asterisks) diverging towards the pith to form a single medullary bundle. bu, axillary bud; le, leaf; lt, leaf trace; mb, medullary bundle; th, thorn. Scale bars: A = 200 μm ; C–D = 50 μm . Stained with astra blue and safranin.

1962), meristematic ring (Balfour and Philipson, 1962), and “extra-fascicular cambium” (de Bary, 1884). Here we demonstrated that the continuous concentric procambium is a peripheral ring of procambial cells that differentiates beneath the innermost cortex layer. The primary origin of these vascular bundles was confirmed due to the presence of vessel elements with annular and helical thickenings (typical of primary xylem, i.e., protoxylem and metaxylem), as also indicated by Inouye (1956).

The polycyclic eustele in Nyctaginaceae

The results on the origin and development of medullary bundles and the continuous concentric procambium are directly related to

the stellar concept. As we have shown, the way that both medullary bundles and the vascular bundles from the continuous concentric procambium are built in most Nyctaginaceae means that they correspond to the primary vascular bundles, which constitute the eustele. Therefore, the concept of polycyclic eustele in Nyctaginaceae should be slightly modified to “medullary bundles arranged within the pith that are surrounded by vascular bundles derived from a continuous concentric procambium”. It is assumed that this organization seems to be a particularity of Nyctaginaceae and other Caryophyllales from the phytolaccoid clade.

Because the polycyclic eustele contains several medullary bundles within the pith, this arrangement of the vascular system in eudicots has long been compared to the “atactostele” of

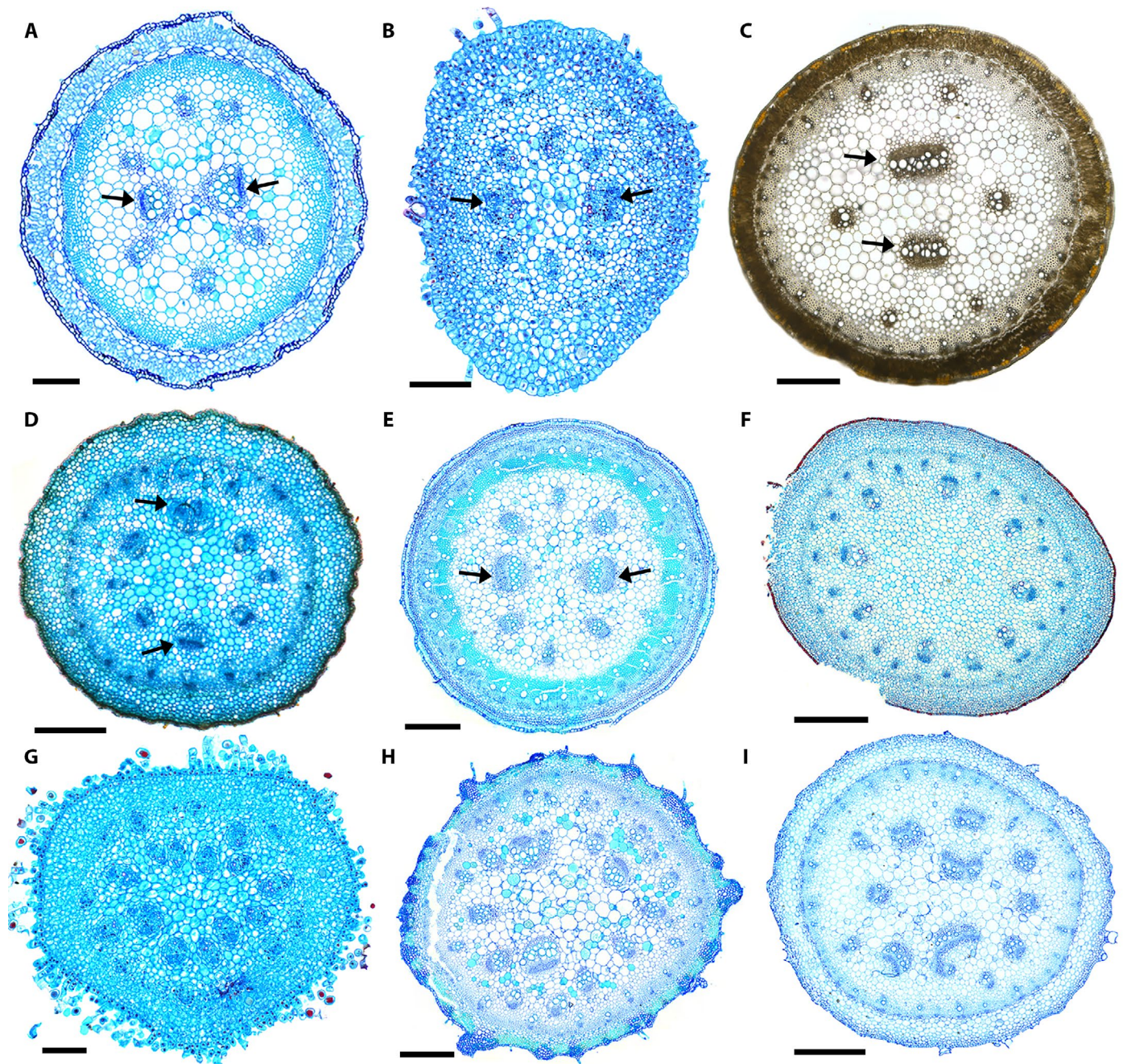


FIGURE 6. Organization and diversity of medullary bundles. (A–E) Type 1, eight medullary bundles organized in a ring. (A) *Acleisanthes chenopodioides*. (B) *Commicarpus scandens*. (C) *Anulocaulis leiosolenus* var. *gypsogenus*. (D) *Guapira laxa*. (E) *Pisoniella arborescens*, illustrating that, for this species, this arrangement is present in primary structure, as well as in stems with secondary growth. (F) Type 2, medullary bundles arranged in two concentric rings, *Colignonia glomerata*. (G–I) Type 3, medullary bundles showing several bundles irregularly distributed. (G) *Bougainvillea berberidifolia*. (H) *Salpianthus purpurascens*. (I) *Nyctaginia capitata*. arrows, larger (central) medullary bundles. Scale bars: A, B, G = 100 μm ; C, D, I = 400 μm ; E, F, H = 300 μm . A, E, G–I, stained with toluidine blue; B, D, F, stained with astra blue and safranin; C, no stain.

the monocots (de Bary, 1884; Wilson, 1924; Pant and Mehra, 1963; Isnard et al., 2012). Although the arrangement of medullary bundles in Nyctaginaceae may be similar in appearance to the stele of monocots, there are differences in origin, development, and structure. Differently from Nyctaginaceae and other plants with medullary bundles, monocots generally possess several bundles seemingly uniformly spaced (i.e., ordered; sensu Korn, 2016), which may be

formed by two types of bundles, the bundles that form leaf traces and cauline (axial) bundles that are not continuous with the leaves (Tomlinson, 1984; Cattai and Menezes, 2010; Botânico and Angyalossy, 2013; Vita et al., 2019).

Another general idea is that the medullary bundles are comparable to the regular bundles (stele bundles) of eudicots, which, during evolution, diverged inward at the nodes (Wilson, 1924; Zamski, 1980; Costea

TABLE 2. Information on the types of arrangement of medullary bundles in relation to other morphological characteristics. The arrangement of medullary bundles was inferred from specimens with “a” and/or “b” in Table 1, since this organization may change with secondary growth. When only the genus name is included, then all species collected in that genus were studied; otherwise, the species name was specified.

Arrangement of medullary bundles in primary growth	Tribe	Taxa	Phyllotaxy	Presence/absence of thorns	Hollow stems	Observations
Type 1 – eight medullary bundles organized in one or two rings; the central ones are larger than the others. See Fig. 6A-6E.	Nyctagineae	<i>Abronia nealleyi</i> , <i>Acleisanthes chenopodioides</i> , <i>Acleisanthes lanceolata</i> , <i>Acleisanthes longiflora</i> , <i>Anulocaulis leiosolenus</i> var. <i>leiosolenus</i> , <i>Allionia incarnata</i> , <i>Boerhavia linearifolia</i> , <i>Commicarpus</i> , <i>Cyphomeris</i> , <i>M. albid</i> a, <i>Okenia</i>	Opposite	–	–	Sometimes one bundle was lacking and only seven constituted the ring, as in <i>Allionia</i> and <i>Cyphomeris</i> . The arrangement is usually lost in fully developed stems due to new bundles.
	Pisonieae	<i>Pisoniella arborescens</i>	Opposite	–	–	There was also one sample with 10 medullary bundles. The arrangement was maintained in developed stems.
Type 2 – ≥ than 10 medullary bundles arranged in two or more rings. Medullary bundles in the inner ring are usually larger. See Fig. 1C, 6F.		<i>Guapira laxa</i> , <i>Guapira pernambucensis</i> , <i>Neea hermaphrodita</i>	Subopposite	–	–	The arrangement is usually lost in fully developed stems due to new bundles.
	Nyctagineae	<i>Mirabilis jalapa</i> , <i>M. aggregata</i> , <i>Mirabilis</i> sp.	Opposite	–	–	The medullary bundles delimit a large pith, which disintegrate later forming a hollow stem. The arrangement was maintained in developed stems.
	Colignonieae	<i>Colignonia glomerata</i>	Opposite	–	+	
Type 3 – ≥ than 10 medullary bundles in a non-specific arrangement. See Fig. 6G-I.	Nyctagineae	<i>Boerhavia herehoensis</i> , <i>B. torreyana</i>	Opposite	–	–	
		<i>Mirabilis viscosa</i>		–	–	
		<i>Nyctaginia</i>		–	–	
	Bougainvilleae	<i>Bougainvillea</i>	Alternate	+	–	
	Boldoeae	<i>Salpianthus purpurascens</i>	Alternate	–	–	
	Pisonieae	<i>Guapira graciliflora</i>	Subopposite	–	–	
	<i>Grajalesia fasciculata</i>	Opposite	–	–		
	<i>Pisonia aculeata</i>	Subopposite	+	–		
	<i>Pisonia</i> sp.2	Subopposite	–	–		

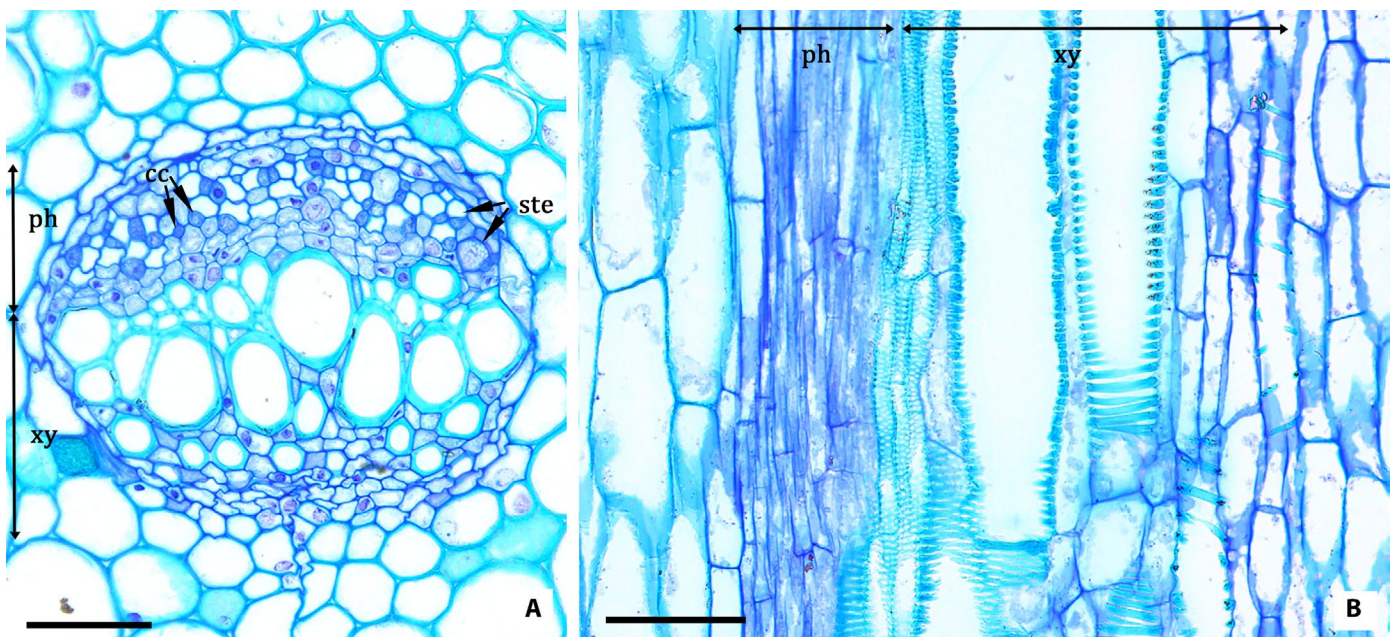


FIGURE 7. Collateral medullary bundles in *Anulocaulis leiosolenus* var. *gypsogenus*. (A) Transverse section. (B) Longitudinal section. cc, companion cell; ph, phloem; ste, sieve-tube element; xy, xylem. Scale bars: 50 μ m. Stained with toluidine blue.

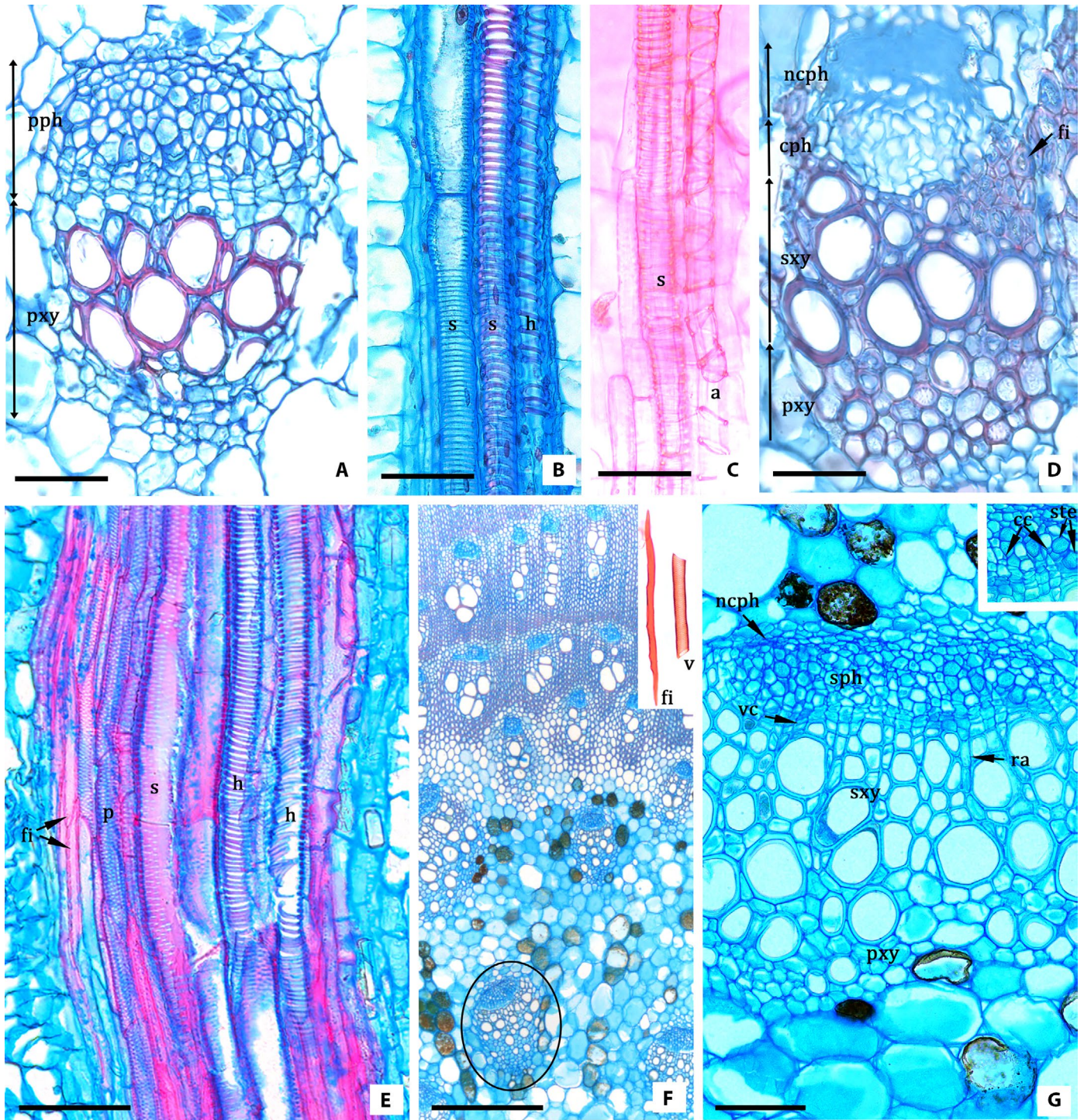


FIGURE 8. Anatomy of medullary bundles. (A, B) *Pisoniella glabrata*, collateral medullary bundles during primary growth. Notice that primary xylem and primary phloem are constituted only of conducting elements and parenchyma. (C) *Colignonia glomerata*, macerated medullary bundles from a sample in primary growth. (D, E) *Guapira laxa*, medullary bundles during secondary growth evidenced by secondary xylem with fibers, secondary phloem, and nonconducting primary phloem. (D) Transverse section. (E) Longitudinal section. Notice fibers, scalariform (s) and pitted vessels (p). (F–G) *Salpianthus purpurascens*. (F) Adult stem showing the presence of functional medullary bundles (ellipse). Macerated fiber and pitted vessel (inset) from medullary bundles during secondary growth. (G) Detail of medullary bundles in secondary growth, evidenced by the secondary xylem, conducting secondary phloem with functional sieve-tube elements and companion cells (inset), vascular ray, and nonconducting phloem at the periphery. a, annular vessel thickening; cc, companion cell; cph, conducting phloem; fi, fiber; h, helical vessel thickening; mb, medullary bundles; ncph, nonconducting phloem; p, pitted vessel; pph, primary phloem; pxy, primary xylem; ra, vascular ray; s, scalariform vessel thickening; sph, secondary phloem; ste, sieve-tube element; sxy, secondary xylem; vc, vascular cambium; v, vessel element. Scale bars: A–D = 50 μ m; E, G = 100 μ m; F = 500 μ m. A–F, stained with astra blue and safranin; G, stained with toluidine blue.

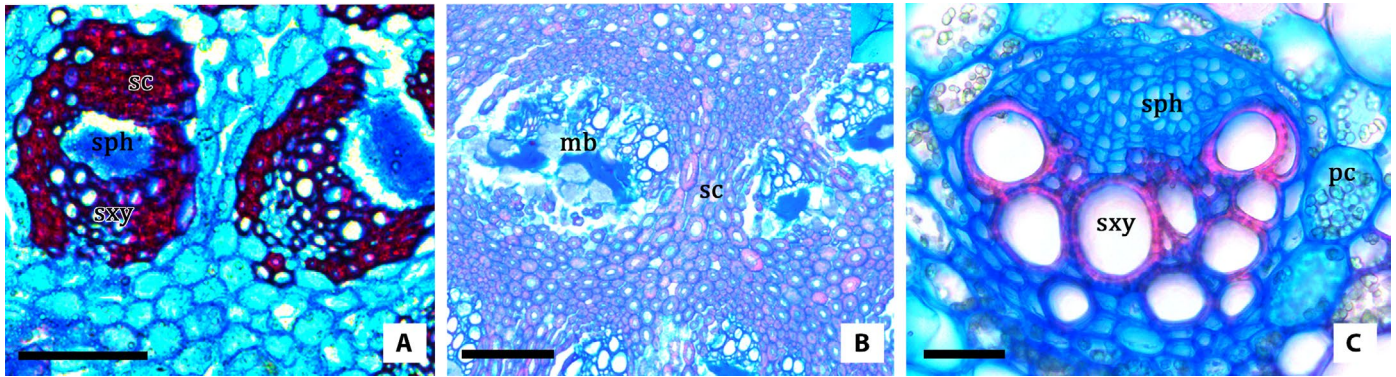


FIGURE 9. Details of medullary bundles in developed stems. (A) *Guapira ligustrifolia*, medullary bundles encircled by a sheath of sclerenchyma. (B) *Phaeoptillum spinosum*, medullary bundles immersed in sclerenchymatic tissue. (C) *Acleisanthes chenopodioides*, medullary bundle encircled by parenchymatic cells containing starch grains. mb, medullary bundle; pc, parenchymatic cell; sc, sclerenchyma; sph, secondary phloem; sxy, secondary xylem. Scale bars: A = 200 μ m; B = 250 μ m; C = 50 μ m. Stained with astra blue and safranin.

and DeMason, 2001). The observations in this study may corroborate this observation, since the medullary bundles in Nyctaginaceae do not form an independent system but rather constitute the primary vascular system, which is formed from leaf and thorn traces. Therefore, analyzing the morphological complexity acquired by the species with polycyclic eustele in Nyctaginaceae, two main developmental shifts are observed: (1) the establishment of leaf-traces in the pith as medullary bundles and (2) the belated appearance of a continuous concentric procambium that forms the ring of vascular bundles that delimits the pith—equivalent to the ring of vascular bundles forming the regular eustele in Leucastereae and eudicots in general.

Arrangement of medullary bundles and their independence from shoot morphology

The presence of medullary bundles is directly related to the formation of lateral organs, since medullary bundles form leaf, branch, and thorn traces. Therefore, a different arrangement of medullary bundles might be expected to arise in direct correlation with the external morphology. However, we found the number and arrangement of medullary bundles in Nyctaginaceae to be independent from the external morphology, such as the different phyllotaxies or the presence or absence of thorns (Table 1). Likewise, the study of Hernández-Ledesma et al. (2011) with 24 species of *Mirabilis* found that the number of medullary bundles varied from 4 to 40 with different organizations, even though all the species exhibit the same phyllotaxy. Similar results are found in other groups, such as for the genus *Piper* (Piperaceae) where seven species of equal phyllotaxy showed a variable number of medullary bundles (Yang and Chen, 2017). Overall, the organization of medullary bundles depends on the proximity of the nodes due to bifurcations or anastomoses that may occur along the medullary bundle's trajectory in the internodes.

An interesting case was found in the genus *Pisoniella*. Investigation of the number and arrangement of medullary bundles showed that the two species of *Pisoniella* have different patterns, despite their similar external morphology. While *P. glabrata* always had around 20 bundles distributed in two to three concentric rings, *P. arborescens* had mostly eight bundles arranged in a single ring. Interestingly, the number and arrangement of medullary bundles in these two species are quite stable and remained constant when

comparing different developmental stages, even among young or adult stems. Although *P. arborescens* and *P. glabrata* have been distinguished as different species by some authors (Fay, 1980; Spellenberg, 2001; Nee, 2004), others have classified the genus as monotypic (Standley, 1911; Bittrich and Kühn, 1993) or consisting of one species divided into two varieties (López and Anton, 2006). As expected, the vegetative and reproductive morphology of these two taxa are very similar, but apparently, they have a disjunct distribution with *P. glabrata* occurring in South America, while *P. arborescens* is restricted to Mexico and Central America. Now, differences in the structure of primary vascular system add additional evidence that these two species should be considered different.

Anatomy of medullary bundles

All medullary bundles in Nyctaginaceae are collateral, as also demonstrated by previous works with the family (Nair and Nair, 1961; Stevenson and Popham, 1973; Mikesell and Popham, 1976). However, other types of medullary bundles have also been reported in eudicots, including amphicribal, inversely oriented, or variations between these patterns (Metcalfe and Chalk, 1950; Davis, 1961).

Later in development, the collateral medullary bundles in Nyctaginaceae increase in size due to the production of secondary tissues (Balfour, 1965; Rajput et al., 2009; this study), as also observed in Apiaceae (Lambeth, 1940), Cactaceae (Mauseth, 1993), and Convolvulaceae (Kapadane et al., 2019). We noticed that the secondary growth in the medullary bundles is synchronous with the secondary growth of the external ring of bundles derived from the continuous concentric procambium. Thus, while the stem increases in diameter, the medullary bundles also continue to produce secondary xylem and secondary phloem to some extent, and their conducting cells maintain function throughout the plant's lifespan. Secondary growth is noticeable due to the presence of a cambium, with the production of fibers, pitted vessels, and the presence of collapsed cells in the phloem, which indicate that new phloem elements have been produced.

Ancestral character state reconstruction of eustele subtypes

The observed differences in distribution of the eustele subtypes is enough to define an entire clade, since the regular eustele is

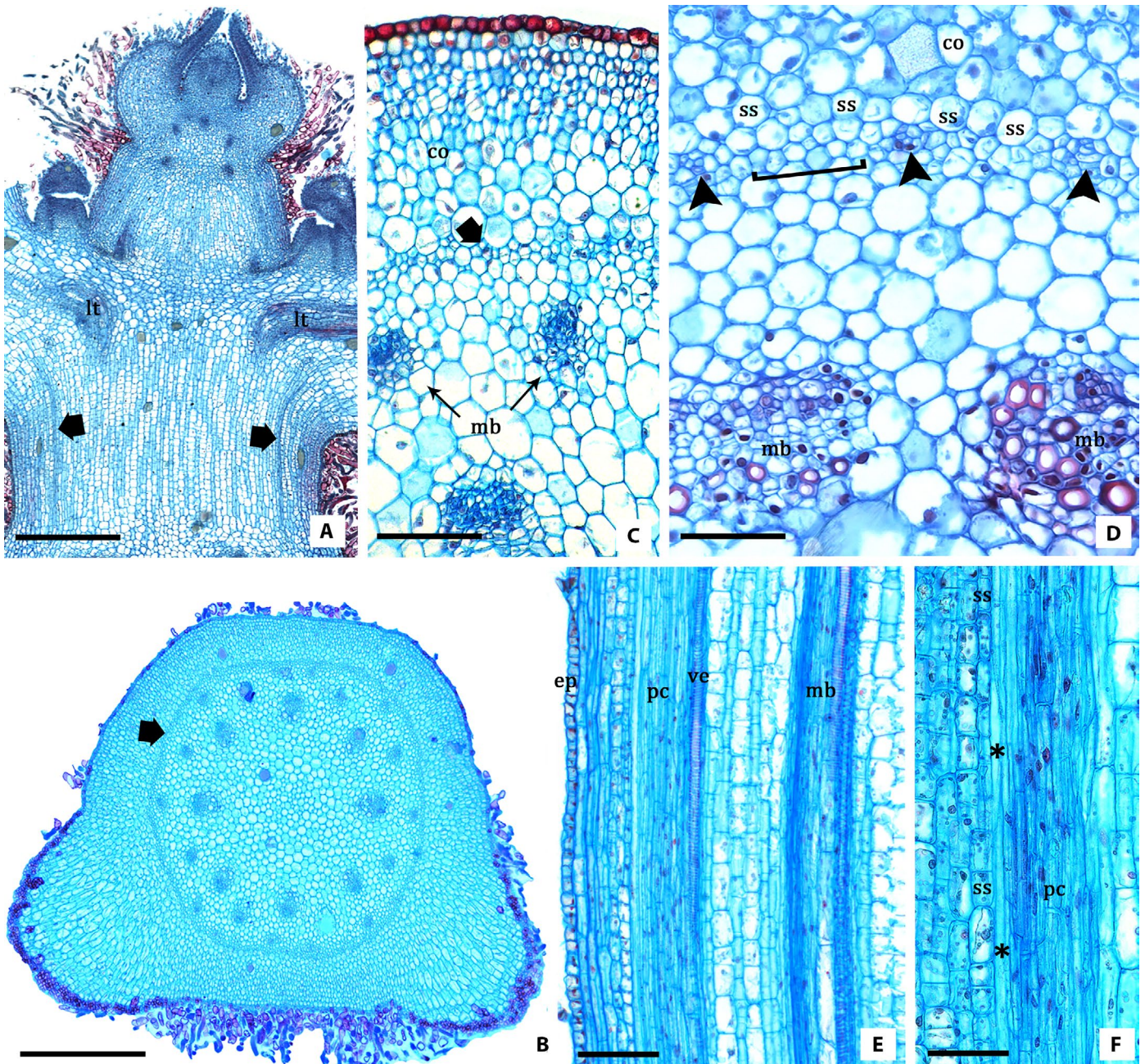


FIGURE 10. Origin and development of continuous concentric procambium. (A–C) *Colignonia glomerata*, view from developing continuous concentric procambium in early developmental stages (arrows). (A) Longitudinal section. (B, C) Transverse sections. (B) General view. (C) Detail of medullary bundles and continuous concentric procambium. (D) *Commicarpus scandens*, continuous concentric procambium cells dividing to form the first vascular elements (arrowhead). (E, F) *Pisoniella glabrata*. (E) Detail of the continuous concentric procambium in a region where a vascular bundle is differentiating. Note the presence of the first differentiated vessel element. (F) Continuous concentric procambium formed by elongated cells that differentiate into vascular bundles and the parenchymatic cells forming the outermost part of the vascular system (asterisks). Bracket, interfascicular region; co, cortex; ep, epidermis; lt, leaf trace; mb, medullary bundle; pc, continuous concentric procambium; ss, starch sheath; ve, vessel element. Scale bars: A, B = 400 μm ; C, E = 100 μm ; D, F = 50 μm . A, C, D, stained with astra blue and safranin; B, E, F, stained with toluidine blue.

exclusive to all the representatives of tribe Lecaustereae and is here suggested as an anatomical synapomorphy of this clade. The exclusive occurrence of regular eustele in tribe Leucaustereae is quite interesting, given that this tribe is also known as having a set of other morphological characteristics differing from other tribes of Nyctaginaceae, e.g., stellate trichomes, absence of

anthocarp (typical fruit of Nyctaginaceae) and bisexual flowers (Bittrich and Kühn, 1993; Douglas and Manos, 2007; Douglas and Spellenberg, 2010; Rossetto et al., 2019). As a result, the occurrence of medullary bundles in the remaining taxa has an important systematic implication at the tribal and generic level within Nyctaginaceae.

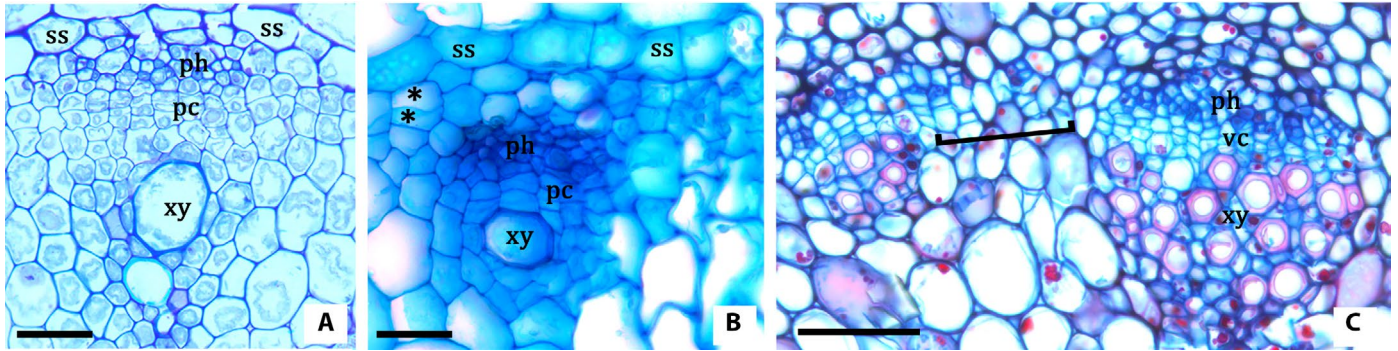


FIGURE 11. Vascular bundles originated from the continuous concentric procambium. (A) *Nyctaginia capitata*, collateral vascular bundle. (B) *Colignonia glomerata*, detail of vascular bundle, outermost cells of vascular system (asterisks) and starch sheath. (C) *Guapira graciliflora*, differentiated vascular bundle evidenced by primary xylem and primary phloem, and interfascicular region (bracket). pc, procambium; ph, phloem; ss, starch sheath; vc, vascular cambium; xy, xylem. Scale bars: A–C = 50 μm. A, stained with toluidine blue; B, C, stained with astra blue and safranin.

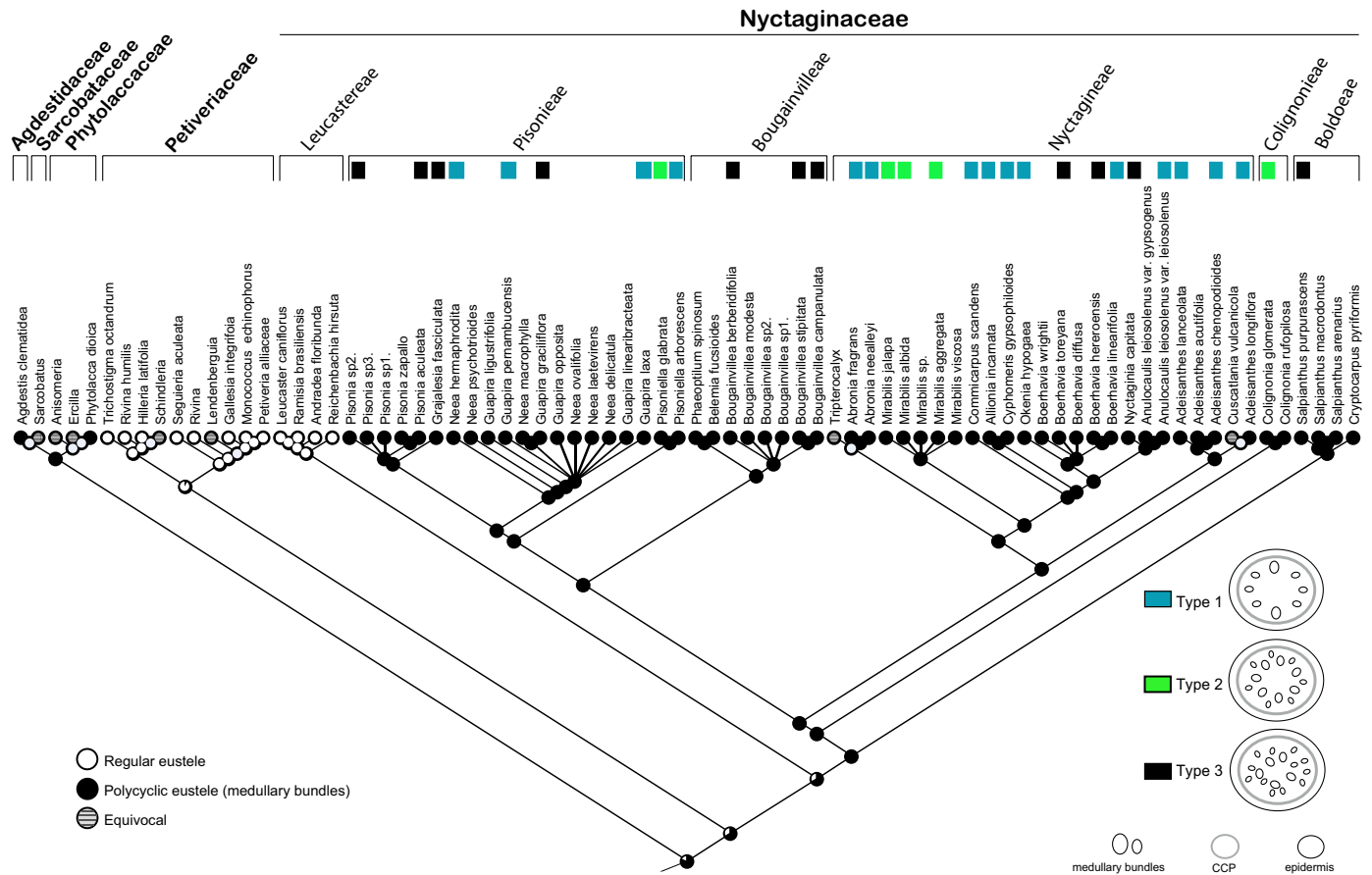


FIGURE 12. Different arrangements of medullary bundles; ancestral character state reconstruction of the presence of medullary bundles in Nyctaginaceae and sister groups. The deepest node inferred 81% probability for presence of medullary bundles (black) versus 19% for absence (white). Nyctaginaceae most recent common ancestor was inferred to have 45% likelihood of being type 3. CCP, continuous concentric procambium.

The ancestral character state reconstruction for the eustele characters within Nyctaginaceae showed that the ancestors for the family likely had a polycyclic eustele. Consequently, the occurrence of a regular eustele in tribe Leucastereae represents a single evolution (autapomorphy) within the Nyctaginaceae. When Nyctaginaceae is put in a larger phylogenetic context, including their sister groups, i.e., Agdestidaceae, Phytolaccaceae,

and Sarcobataceae, the sister groups of Nyctaginaceae, which all except Petiveriaceae share the presence of medullary bundles, it becomes evident that the most recent common ancestor of this entire clade is likewise reconstructed as having a polycyclic eustele. Therefore, the presence of regular eustele in tribe Leucastereae and the family Petiveriaceae reconstructs as a reversal (an independent evolution) to the character

state ancestral for all lignophytes (the clade including extinct progymnosperms, gymnosperms, and angiosperms, all having a bifacial vascular cambium), which is thought to be a regular eustele, while the presence of a polycyclic eustele in Nyctaginaceae and close-related families likely constitutes a synapomorphy for the phytolaccoid clade and symplesiomorphy for Nyctaginaceae.

Three configurations for the polycyclic eustele were encountered. Our results showed that the ancestor of Nyctaginaceae probably had a polycyclic eustele with more than or 10 medullary bundles in a nonspecific arrangement (type 3), with multiple evolution of types 1 (8 medullary bundles in symmetrical groups) and 2 (≥ 10 medullary bundles in two to three concentric rings) during the evolutionary history of this character. Considering this reconstructed likelihood, the shifts that led to the appearance of type 2 simply represented a change in the disposition of the medullary bundles resulting in the formation of rings. On the other hand, the evolution of type 1 would entail a reduction in the number of medullary bundles and their organization in groups. The number and organization of medullary bundles is diverse in Nyctaginaceae, but their occurrence is widespread and independent from phyllotaxy, habit, and habitat. Except for the prevalence of type 1 within Nyctagineae, a lineage composed mostly by herbs or subshrubs, no other pattern emerged among the clades.

Medullary bundles have apparently evolved not only in the phytolaccoid clade, but also independently in other families within the Caryophyllales, both among the core families, such as Amaranthaceae and Cactaceae and in the noncore Caryophyllales, as in Nepenthaceae (Metcalf and Chalk, 1950; Mauseth, 1993; Schwallier et al., 2017). Among these families, the medullary bundles have been investigated in the families Nepenthaceae and Cactaceae. In the first, Schwallier et al. (2017) reported that it is a derived feature, which evolved multiple times independently, although it is present only in eight of the 40 species investigated. For the latter, Mauseth (1993) found that they appear to be relictually absent in the family, originating during early stages of evolution of subfamily Cactoideae.

CONCLUSIONS

The medullary bundles share the same origin and development across Nyctaginaceae, except for representatives of tribe Leucastereae where they are absent. Our observations showed that the number and organization of medullary bundles in stem cross section are unrelated to phyllotaxy, habit, and habitat. Given the presence or absence of medullary bundles, the primary vascular system of Nyctaginaceae can be subdivided in two subtypes of eustele: the polycyclic eustele and the regular eustele. Here, we showed that their absence is inferred as a potential synapomorphy of tribe Leucastereae. Although we have revealed the character history of medullary bundles for Nyctaginaceae, their evolution across Caryophyllales requires further investigation. Information on the evolution of medullary bundles for the order is of interest given that they are present in several families both in the core and noncore Caryophyllales. Their occurrence in the close relatives of Nyctaginaceae, for instance, resulted in the inference of medullary bundles as a symplesiomorphy for Nyctaginaceae and a synapomorphy for the phytolaccoid clade. Whether the same developmental genetic pathways (deep homology) are responsible for the

presence of medullary bundles in other Caryophyllalean families is something to be addressed in future studies.

ACKNOWLEDGMENTS

This study was financed in part by the Coordenação de Aperfeiçoamento de Pessoal de Nível Superior–Brasil (CAPES), Finance Code 001 and Papiit (IA200319). We thank Fundação de Amparo à Pesquisa do Estado de São Paulo for the Ph.D. grant to I.L.C.N. (FAPESP, Proc. 2017/17107-3) and the U.S. National Science Foundation for funding for M.J.M. (DEB 1054539). We also thank the Smithsonian Institution for the Cuatrecasas award to I.L.C.N. and authorization to sample from the herbarium (US) and wood collection (USw), the U.S.D.A. Forest Products Laboratory (Alex C. Wiedenhoft and Adriana Costa) for providing specimens from their wood collection (MADw). We thank Felipe Rossetto for constructive discussions and Juliana Pimentel for helping to process *Allionia* specimens. We are grateful to the Plant Anatomy Laboratory of USP and the Laboratory of Microtomography at the Institute of Biosciences of USP for technical support, the personnel who helped us in collections in Bolivia (Romel Nina), Brazil (Efigênia de Melo and Felipe Rossetto), Mexico (Alejandro Torres-Montúfar and Camille Truong), and the United States (Patrick Alexander). We thank the Editor-in-Chief Pamela Diggle, the Associate Editor, and three anonymous reviewers for their careful revisions and suggestions to improve this paper.

AUTHOR CONTRIBUTIONS

I.L.C.N. and V.A. conceived the research; I.L.C.N., M.R.P., N.A.D., M.H.N., C.F.C.S., and M.J.M. assisted in plant collection; I.L.C.N. performed anatomical procedures, phylogenetic comparative analysis and wrote the manuscript; M.J.M. and N.A.D. provided the phylogenetic tree; I.L.C.N., M.R.P., and V.A. analyzed and interpreted the results; all authors revised, complemented, and corrected the text and gave final approval for publication.

DATA AVAILABILITY

Supplementary data are available online at FigShare (Table S1: Character and character states for ancestral reconstructions of medullary bundles in Nyctaginaceae and related families, <https://doi.org/10.6084/m9.figshare.11815260>; Fig. S1: Diversity of medullary bundles in stems of Nyctaginaceae species, <https://doi.org/10.6084/m9.figshare.11815209.v2>).

LITERATURE CITED

- Angyalossy, V., G. Angeles, M. R. Pace, A. C. Lima, C. L. Dias-Leme, L. G. Lohmann, and C. Madero-Vega. 2012. An overview on the anatomy, development and evolution of the vascular system of lianas. *Plant Ecology and Diversity* 5: 167–182.
- Angyalossy, V., G. Angeles, M. R. Pace, and A. C. Lima. 2015. Liana anatomy: a broad perspective on structural evolution of the vascular system. In S. A. Schnitzer, F. Bongers, R. Burnham, and F. E. Putz [eds.], *Ecology of lianas*, 253–287. Wiley-Blackwell, Oxford, UK.

- Angyalossy, V., M. R. Pace, R. F. Evert, C. R. Marcatti, A. A. Oskolski, T. Terrazas, E. Kotina, et al. 2016. IAWA list of microscopic bark features. *IAWA Journal* 37: 517–615.
- Balfour, E. 1965. Anomalous secondary thickening in Chenopodiaceae, Nyctaginaceae and Amaranthaceae. *Phytomorphology* 15: 111–122.
- Balfour, E. E., and W. R. Philipson. 1962. The development of the primary vascular system of certain dicotyledons. *Phytomorphology* 12: 110–143.
- Barbosa, A. C. F., M. R. Pace, L. Witovisk, and V. Angyalossy. 2010. A new method to obtain good anatomical slides of heterogeneous plant parts. *IAWA Journal* 31: 373–383.
- Barbosa, A. C. F., G. R. O. Costa, V. Angyalossy, T. C. Santos, and M. R. Pace. 2018. A simple and inexpensive method for sharpening permanent steel knives with sandpaper. *IAWA Journal* 39: 373–383.
- Beck, C. B. 2010. An introduction to plant structure and development. Cambridge University Press, Cambridge, UK.
- Beck, C. B., R. Schmid, and G. W. Rothwell. 1982. Stellar morphology and the primary vascular system of seed plants. *Botanical Review* 48: 691–815.
- Berlyn, G. P., and J. P. Miksche. 1976. Botanical microtechnique and cytochemistry. Iowa State University Press, Ames, Iowa, USA.
- Bittrich, V., and U. Kühn. 1993. Nyctaginaceae. In K. Kubitzki, J. G. Rohwer, and V. Bittrich [eds.], The families and genera of flowering plants, vol. 2, 473–486. Springer, Berlin, Germany.
- Boke, N. H. 1941. Zonation in the shoot apices of *Trichocereus spachianus* and *Opuntia cylindrica*. *American Journal of Botany* 28: 656–664.
- Botânico, M. P., and V. Angyalossy. 2013. Is the secondary thickening in palms always diffuse? *Anais da Academia Brasileira de Ciências* 85: 1461–1472.
- Bukatsch, F. 1972. Bemerkungen zur Doppelfärbung Astrablau-Safranin. *Mikrokosmos* 61: 255.
- Carlquist, S. 1999. Wood anatomy of *Agdestis* (Caryophyllales): systematic position and nature of the successive cambia. *Aliso* 18: 35–43.
- Carlquist, S. 2000. Wood anatomy of phytolaccoid and rivinoid Phytolaccaceae (Caryophyllales): ecology, systematics, nature of successive cambia. *Aliso* 19: 13–29.
- Carlquist, S. 2001. Comparative wood anatomy. Systematic, ecological and evolutionary aspects of dicotyledon wood. 2nd ed. Springer Verlag, Berlin, Germany.
- Cattai, M. B., and N. L. Menezes. 2010. Primary and secondary thickening in the stem of *Cordyline fruticosa* (Agavaceae). *Anais da Academia Brasileira de Ciências* 82: 653–662.
- Costea, M., and D. A. DeMason. 2001. Stem morphology and anatomy in *Amaranthus* L. (Amaranthaceae) taxonomic significance. *Journal of the Torrey Botanical Society* 128: 254–281.
- Davis, E. L. 1961. Medullary bundles in the genus *Dahlia* and their possible origin. *American Journal of Botany* 48: 108–113.
- de Bary, A. 1884. Comparative anatomy of the vegetative organs of the phanerogams and ferns. Clarendon Press, Oxford, UK.
- Douglas, N. A., and P. S. Manos. 2007. Molecular phylogeny of Nyctaginaceae: taxonomy, biogeography, and characters associated with a radiation of xerophytic genera in North America. *American Journal of Botany* 94: 856–872.
- Douglas, N. A., and R. Spellenberg. 2010. A new tribal classification of Nyctaginaceae. *Taxon* 59: 905–910.
- Duarte, M. R., and J. F. Lopes. 2005. Leaf and stem morphoanatomy of *Petiveria alliacea*. *Fitoterapia* 76: 599–607.
- Eames, A. J., and L. H. MacDaniels. 1925. An introduction to plant anatomy. McGraw-Hill, New York, NY, USA.
- Esau, K. 1954. Primary vascular differentiation in plants. *Biological Reviews of the Cambridge Philosophical Society* 29: 46–86.
- Esau, K. 1967. Plant anatomy. John Wiley, New York, NY, USA.
- Fay, J. J. 1980. Nyctaginaceae. In A. Gómez-Pompa [ed.], Flora de Veracruz, fasc. 13, 1–54. Instituto Nacional de Investigaciones sobre Recursos Bióticos, Xalapa, México.
- Gibson, A. C. 1994. Vascular tissues. In H. D. Behnke and T. J. Mabry [eds.], Caryophyllales. Evolution and systematics, 45–74. Springer-Verlag, Berlin, Germany.
- Hayden, S. M., and W. J. Hayden. 1994. Stem development, medullary bundles, and wood anatomy of *Croton glandulosus* var. *septentrionalis* (Euphorbiaceae). *IAWA Journal* 15: 51–63.
- Hearn, D. J. 2009. Developmental patterns in anatomy are shared among separate evolutionary origins of stem succulent and storage root-bearing growth habits in *Adenia* (Passifloraceae). *American Journal of Botany* 96: 1941–1956.
- Hernández-Ledesma, P., T. Terrazas, and H. Flores-Olvera. 2011. Comparative stem anatomy of *Mirabilis* (Nyctaginaceae). *Plant Systematics and Evolution* 292: 117–132.
- Hernández-Ledesma, P., W. G. Berendsohn, T. Borsch, S. Von Mering, H. Akhiani, S. Arias, I. Castaneda-Noa, et al. 2015. A taxonomic backbone for the global synthesis of species diversity in the angiosperm order Caryophyllales. *Willdenowia* 45: 281–383.
- Holwill, P. J. A. 1950. Occurrence of medullary bundles in the apple shoot. *Nature* 165: 156–157.
- Inouye, R. 1956. Anatomical studies on the vascular system of *Mirabilis jalapa* L. *Botanical Magazine* 69: 554–559.
- Isnard, S., J. Prosperi, S. Wanke, S. T. Wagner, M. S. Samain, S. Trueba, L. Frenze, et al. 2012. Growth form evolution in Piperales and its relevance for understanding angiosperm diversification: an integrative approach combining plant architecture, anatomy, and biomechanics. *International Journal of Plant Sciences* 173: 610–639.
- Jansen, S., L. P. Ronse Decraene, and E. Smets. 2000. On the wood and stem anatomy of *Monococcus echinophorus* (Phytolaccaceae s.l.). *Systematics and Geography of Plants* 70: 171–179.
- Johansen, D. A. 1940. Plant microtechnique. McGraw-Hill, New York, NY, USA.
- Kapadane, K. K., R. A. Shelke, A. D. Gondaliya, and K. S. Rajput. 2019. Formation of medullary phloem in *Argyrea nervosa* (Burm. f.) Bojer. *Plant Science Today* 6: 151–159.
- Kirchoff, B. K., and A. Fahn. 1984. Initiation and structure of the secondary vascular system in *Phytolacca dioica* (Phytolaccaceae). *Canadian Journal of Botany* 62: 2432–2440.
- Korn, R. W. 2016. Vascular architecture of the monocot *Cyperus involucreatus* Rottb. (Cyperaceae). *SpringerPlus* 5: 4.
- Lambeth, E. C. 1940. Ontogeny of medullary bundles in *Apium graveolens*. *Botanical Gazette* 102: 400–405.
- López, H. A., and A. M. Anton. 2006. Nyctaginaceae. In A. M. Anton [ed.], Flora fanerogámica Argentina, 1–22. Programa Proflora, Córdoba, Argentina.
- Lucansky, W. T. 1974. Comparative studies of the nodal and vascular anatomy in the Neotropical Cyatheaceae. I. *Metaxya* and *Lophosoria*. *American Journal of Botany* 61: 464–471.
- MacDougal, D. T. 1926. Growth and permeability of century-old cells. *American Naturalist* 60: 393–415.
- Maddison, W. P., and D. R. Maddison. 2009. Mesquite: a modular system for evolutionary analysis, version 3.6. Website: <http://mesquiteproject.org>.
- Males, J. 2017. Secrets of succulence. *Journal of Experimental Botany* 68: 2121–2134.
- Mauseth, J. D. 1988. Plant anatomy. Benjamin and Cummings, Menlo Park, CA, USA.
- Mauseth, J. D. 1993. Medullary bundles and the evolution of cacti. *American Journal of Botany* 80: 928–932.
- Mauseth, J. D. 2006. Structure–function relationships in highly modified shoots of Cactaceae. *Annals of Botany* 98: 901–926.
- Metcalfe, C. R., and L. Chalk. 1950. Anatomy of the dicotyledons: leaves, stems, and wood in relation to taxonomy with notes on economic uses. Clarendon Press, Oxford, UK.
- Mikesell, J. E., and R. A. Popham. 1976. Ontogeny and correlative relationships of the primary thickening meristem in four-o'clock plants (Nyctaginaceae) maintained under long and short photoperiods. *American Journal of Botany* 63: 427–437.
- Nair, N. C., and V. J. Nair. 1961. Studies on the morphology of some members of the Nyctaginaceae I, Nodal anatomy of *Boerhavia*. *Proceedings of the Indian Academy of Science* 54: 281–294.

- Nee, M. H. 2004. Flora de la región del Parque Nacional Amboró, Bolivia, vol. 2, Magnoliidae, Hamamelidae y Caryophyllidae. Editorial FAN, Santa Cruz, Bolivia.
- O'Brien, T. P., N. Feder, and M. E. McCully. 1964. Polychromatic staining of plant cell walls by toluidine blue O. *Protoplasma* 59: 368–373.
- Ogburn, R. M., and E. J. Edwards. 2013. Repeated origin of three-dimensional leaf venation releases constraints on the evolution of succulence in plants. *Current Biology* 23: 722–726.
- Ogura Y. 1927. Comparative anatomy of Japanese Cyatheaaceae. Journal of the Faculty of Science. *Imperial University of Tokyo (Botany)* 1: 141–350.
- Ogura, Y. 1972. Comparative anatomy of vegetative organs of the pteridophytes. 2nd ed. Gebrüder Borntraeger, Berlin, Germany.
- Pant, D. D., and S. Bhatnagar. 1975. Morphological studies in *Argyrea* Lour. (Convolvulaceae). *Botanical Journal of the Linnean Society* 70: 45–69.
- Pant, D. D., and B. Mehra. 1961. Nodal anatomy of *Boerhaavia diffusa* L. *Phytomorphology* 11: 384–405.
- Pant, D. D., and B. Mehra. 1963. Nodal anatomy of *Bougainvillea glabra* Choisy, *B. spectabilis* Willd. and *Abronia elliptica* Nelson. *Proceedings of the National Institute of Sciences of India* 4: 434–466.
- Pugliali, H. R. L., and O. Marquete. 1989. *Rivina humilis* L. (Phytolaccaceae), anatomia da raiz, caule e folha. *Rodriguésia* 67: 35–43.
- Pulawska, Z. 1972. General and peculiar features of vascular organization and development in shoots of *Bougainvillea glabra* Choisy (Nyctaginaceae). *Acta Societatis Botanicorum Poloniae* 41: 39–70.
- Raj, D. N., and S. P. Nagar. 1980. On medullary bundles of *Achyranthes aspera* L. *Flora* 169: 530–534.
- Raj, D. N., and S. P. Nagar. 1989. Primary vascular differentiation in *Achyranthes aspera* L. *Flora* 183: 327–335.
- Rajput, K. S., V. S. Patil, and K. K. Kapadane. 2009. Structure and development of secondary thickening meristem in *Mirabilis jalapa* (Nyctaginaceae). *Polish Botanical Journal* 54: 113–121.
- Rossetto, E. F. S., A. D. Faria, C. F. Ruas, N. A. Douglas, and J. E. L. S. Ribeiro. 2019. Clarifying generic delimitation in the tribe Pisonieae (Nyctaginaceae), after more than a century of taxonomic confusion. *Botanical Journal of the Linnean Society* 189: 378–396.
- Sabnis, T. S. 1921. The physiological anatomy of the plants of Indian desert. *Journal of Indian Botanical Society* 2: 101–102.
- Schmid, R. 1982. The terminology and classification of steles: historical perspective and the outlines of a system. *Botanical Review* 48: 814–931.
- Schwallier, R., B. Gravendeel, H. de Boer, S. Nylander, B. J. van Heuven, A. Sieder, S. Sumail, et al. 2017. Evolution of wood anatomical characters in *Nepenthes* and close relatives of Caryophyllales. *Annals of Botany* 119: 1179–1193.
- Sharma, H. P. 1962. Contributions to the morphology of the Nyctaginaceae. I. Anatomy of the node and inflorescence of some species. *Proceedings of the National Institute of Sciences of India* 56: 35–50.
- Spellenberg, R. 2001. Nyctaginaceae. In G. C. de Rzedowski and J. Rzedowski [eds.], *Flora del Bajío y de regiones adyacentes*, fasc. 93. Instituto de Ecología, Centro Regional del Bajío, Consejo Nacional de Ciencia y Tecnología y Comisión Nacional para el Conocimiento y Uso de la Biodiversidad, Pátzcuaro, México.
- Standley, P. C. 1911. The Allioniaceae of Mexico and Central America. *Contributions from the United States National Herbarium* 13: 377–430.
- Stevens, P. F. 2001 onward. Angiosperm phylogeny website, version 14, July 2012 [and more or less continuously updated since]. Website: www.mobot.org/MOBOT/research/APweb/ [accessed 10 May 2019].
- Stevenson, D. W., and R. A. Popham. 1973. Ontogeny of the primary thickening meristem in seedlings of *Bougainvillea spectabilis*. *American Journal of Botany* 60: 1–9.
- Terrazas, T., and S. Arias. 2002. Comparative stem anatomy in the subfamily Cactoideae. *Botanical Review* 68: 444–473.
- Tomlinson, P. B. 1984. Development on the stem conducting tissues in monocotyledons. In R. A. White and W. C. Dickison [eds.], *Contemporary problems in plant anatomy*, 1–50. Academic Press, London, UK.
- Tomlinson, P. B., and J. B. Fisher. 2000. Stem vasculature in climbing monocotyledons: a comparative approach. In K. L. Wilson and D. A. Morrison [eds.], *Monocotyledons: systematics and evolution*, 89–97. CSIRO, Melbourne, Australia.
- Trueba, S., N. P. Rowe, C. Neinhuis, S. Wanke, S. T. Wagner, and S. Isnard. 2015. Stem anatomy and the evolution of woodiness in Piperales. *International Journal of Plant Science* 176: 468–485.
- Vita, R. S. B., N. L. Menezes, M. O. O. Pellegrini, and G. F. A. Melo-de-Pinna. 2019. A new interpretation on vascular architecture of the cauline system in Commelinaceae (Commelinales). *PLoS One* 14: e0218383.
- Yang, S. Z., and P. H. Chen. 2017. Cambial variations of *Piper* (Piperaceae) in Taiwan. *International Journal of Botany Studies* 58: 1–9.
- Walker, J. F., Y. Yang, T. Feng, A. Timonedá, J. Mikenas, V. Hutchison, C. Edwards, et al. 2018. From cacti to carnivores: Improved phylotranscriptomic sampling and hierarchical homology inference provide further insight into the evolution of Caryophyllales. *American Journal of Botany* 105: 446–462.
- Wilson, C. L. 1924. Medullary bundle in relation to primary vascular system in Chenopodiaceae and Amaranthaceae. *Botanical Gazette* 78: 175–199.
- Worsdell, W. C. 1915. The origin and meaning of medullary (intraxylary) phloem in the stems of dicotyledons. I. Cucurbitaceae. *Annals of Botany* 29: 567–590.
- Zamski, E. 1980. Vascular continuity in the primary and secondary stem tissues of *Bougainvillea* (Nyctaginaceae). *Annals of Botany* 45: 561–567.

APPENDIX 1. Species name for all studied Nyctaginaceae (divided by tribes) and the outgroups. The information includes vouchers followed by the abbreviations for herbaria where the samples are deposited, geographical region, and herbaria/wood collections where specimens were obtained. Herbaria: FLAS, Florida Museum of Natural History; HURB, Universidade Federal do Recôncavo da Bahia; MEXU, Universidad Nacional Autónoma de México; MW, Moscow State University; RB, Jardim Botânico do Rio de Janeiro; SPF, Universidade de São Paulo; US, Smithsonian Institution; USZ, Museo de Historia Natural Noel Kempff Mercado, Universidad Autónoma Gabriel René Moreno.

Species name, *Collector/collector number* (Herbarium), *Collection site*.

Tribe Nyctagineae

Abronia fragrans Nutt. ex Hook., *Douglas 2290* (FLAS), Las Cruces, New Mexico, USA. *Abronia nealleyi* Standl., *Douglas 2281*, (FLAS) Eddy County, Yeso Hills, New Mexico, USA. *Acleisanthes acutifolia* Standl., *US 842034*, Coahuila, Mexico. *Acleisanthes chenopodioides* (A.Gray) R.A.Levin., *Douglas 2289, 2293* (FLAS), Las Cruces, New Mexico, USA. *Acleisanthes lanceolata* (Wootton) R.A.Levin., *Douglas 2277* (FLAS), Malone Mountains, Sierra Blanca, Texas, USA. *Acleisanthes longiflora* A.Gray., *Douglas 2279* (FLAS), Malone Mountains, Sierra Blanca, Texas, USA. *Allionia choisyi* Standl., *US 498327*, New Mexico, USA; *Allionia incarnata* L., *Nee 64124-64126*, (USZ), Parque Nacional Amboró, Pampa Grande, Santa Cruz, Bolivia; *Douglas 2293* (FLAS), Las Cruces, New Mexico, USA. *Anulocaulis leiosolenus* (Torr.) Standl. var. *leiosolenus*, *Douglas 2278* (FLAS), Malone Mountains, Sierra Blanca, Texas, USA. *Anulocaulis leiosolenus* var. *gypsogenus* (Waterf.) Spellenb. & Wootten, *Douglas 2280* (FLAS) Eddy County, Yeso Hills, New Mexico, USA; *Douglas 2283* (FLAS), Crest of 7 Rivers Hills, New Mexico, USA. *Boerhavia diffusa* L., *Pace 753* (MEXU, US), Veracruz, Mexico. *Boerhavia hereroensis* Heimerl., *Sukhorukov 517* (MW), Namib Desert, Karas Region, Namibia. *Boerhavia linearifolia* A.Gray., *Douglas 2284* (FLAS), New Mexico, USA. *Boerhavia torreyana* (S. Watson) Standl., *Douglas 2294* (FLAS), Las Cruces, New Mexico, USA. *Boerhavia wrightii* A.Gray., *Douglas 2288* (FLAS), Las Cruces, New Mexico, USA. *Commicarpus scandens* (L.) Standl., *Acevedo-Rodríguez 16250* (US), Tonalá, Oaxaca, Mexico; *Douglas 2291* (FLAS), New Mexico, USA. *Cyphomeris gypsophiloides* (M. Martens & Galeotti) Standl., *Douglas 2287* (FLAS), Organ Mountains-Desert Peaks National Monument, Las Cruces, New Mexico, USA. *Mirabilis* sp., *Pace 730* (MEXU), Ixmiquilpan, Hidalgo, Mexico. *Mirabilis aggregata* (Ortega) Cav., *Pace 728* (MEXU, US), Ixmiquilpan, Hidalgo, Mexico. *Mirabilis* cf. *albida* (Walter) Heimerl., *Douglas 2286* (FLAS), New Mexico, USA. *Mirabilis jalapa* L., *Acevedo-Rodríguez 16480* (US), Veracruz, Mexico. *Mirabilis viscosa* Cav., *Pace 727* (MEXU), Ixmiquilpan, Hidalgo, Mexico. *Nyctaginia*

capitata Choisy., *Douglas* 2282 (FLAS), New Mexico, USA. *Okenia hypogaea* Schlttdl. & Cham., *Pace* 749 (MEXU, SPF, US), Veracruz, Mexico.

Tribe Pisonieae

Grajesia fasciculata (Standl.) Miranda., *Pace* 765 (MEXU, SPF, US), Chiapas, Mexico. *Guapira linearibracteata* (Heimerl) Lundell., *USw* 29941, Belize. *Guapira pernambucensis* (Casar.) Lundell., *Cunha Neto* 04-05 (HURB), Alagoinhas, Bahia. *Guapira graciliflora* (Mart. ex J.A.Schmidt) Lundell., *Cunha Neto* 06 (HURB), Alagoinhas, Bahia. *Guapira laxa* (Netto) Furlan., *Cunha Neto* 08 (HURB), Universidade Estadual de Feira de Santana, Feira de Santana, Bahia. *Guapira ligustrifolia* (Heimerl) Lundell., *USw* 1886, San Gabriel Island, República Dominicana; *USw* 1982, Hispaniola Island, República Dominicana. *Guapira opposita* (Vell.) Reitz., *Cunha Neto* 07 (HURB), Alagoinhas, Bahia. *Neea delicatula* Standl., *Pace* 689 (US), Reserva Biológica La Selva, Sarapiquí, Heredia, Costa Rica. *Neea hermaphrodita* S.Moore, *Nee* 64112 (USZ), Living Collection Jardín Botánico Municipal de Santa Cruz de la Sierra, Santa Cruz de la Sierra, Bolivia. *Neea laetevirens* Standl., *Pace* 713, 716 (US), Reserva Biológica La Selva, Sarapiquí, Heredia, Costa Rica; *USw* 16154, Los Santos, Panamá. *Neea macrophylla* Britton ex Rusby., *USw* 40851, San Martín, Peru. *Neea ovalifolia* Spruce ex J.A. Schmidt, *USw* 42783, Régina, French Guiana. *Neea psychotrioides* Donn. Sm., *Pace* 763 (MEXU), Estación de Biología Tropical Los Tuxtlas, Veracruz, Mexico; *USw* 29939, Belize. *Pisonia* sp1., *Nee* 64108 (USZ), Living Collection Jardín Botánico Municipal de Santa Cruz de la Sierra, Santa Cruz de la Sierra, Bolivia. *Pisonia* sp2., *Nee* 64132 (USZ), Parque Nacional Amboró, Vallegrande, Santa Cruz, Bolivia. *Pisonia* sp3., *Pace* 789 (MEXU), Puente Nacional, Veracruz, Mexico. *Pisonia aculeata* L., *Acevedo-Rodríguez* 16549 (US), Bonito, Mato Grosso do Sul, Brazil. *Pisonia zapallo* Griseb., *Nee* 64110 (USZ), Living Collection Jardín Botánico Municipal de Santa Cruz de la Sierra, Santa Cruz de la Sierra, Bolivia. *Pisoniella arborescens* (Lag. & Rodr.) Standl., *Pace* 738-739 (MEXU, SPF, US), Alfajayucan, Hidalgo, Mexico. *Pisoniella glabrata* (Heimerl) Standl., *Nee* 64137, 64151 (USZ), Parque Nacional Amboró, Vallegrande, Santa Cruz, Bolivia.

Tribe Bougainvilleae

Belemia fuscoides Pires., *Farney* 4887, 4888 (RB). *Bougainvillea* sp1., *Nee* 64176 (USZ), Rio Grande, Santa Cruz de la Sierra, Bolivia. *Bougainvillea* sp2., *Nee* 64182 (USZ), Rio Grande, Santa Cruz de la Sierra, Bolivia. *Bougainvillea berberidifolia* Heimerl., *Nee* 64140 (USZ), Parque Nacional Amboró, Comarapa, Santa Cruz, Bolivia. *Bougainvillea campanulata* Heimerl., *Acevedo-Rodríguez* 16772 (US), Mato Grosso do Sul, Brazil; *Nee* 64142 (USZ), Parque Nacional Amboró, Comarapa, Santa Cruz, Bolivia. *Bougainvillea*

modesta Heimerl., *Nee* 64115 (USZ), Living Collection Jardín Botánico Municipal de Santa Cruz de la Sierra, Santa Cruz de la Sierra, Bolivia. *Bougainvillea stipitata* Griseb., *Nee* 64121 (USZ), Parque Nacional Amboró, Samaipata, Santa Cruz, Bolivia. *Bougainvillea spectabilis* Willd., *Rossetto* 453 (RB), Estrada Carlos Chagas-Teófilo Otoni, Minas Gerais, Brazil. *Phaeoptilum spinosum* Radlk., *MADw* 37340, Mocamedes, Angola.

Tribe Colignonieae

Colignonia glomerata Griseb., *Nee* 64157-64159 (USZ), Parque Nacional Amboró, Samaipata, Santa Cruz, Bolivia. *Colignonia rufopilosa* Kuntze, *Nee* 64061 (USZ), Cochabamba, Bolivia.

Tribe Boldoeae

Cryptocarpus pyriformis Kunth, *US* 2833648, Galápagos. *Salpianthus arenarius* Bonpl., *US* 1893480, Vallecitos, Mexico. *Salpianthus macrodontus* Standl., *US* 2219249, Sinaloa, Mexico. *Salpianthus purpurascens* (Cav. ex Lag.) Hook. & Arn., *Pace* 774 (MEXU, SPF, US), El Cobanal, Chiapas, Mexico.

Tribe Leucastereae

Andradea floribunda Allemão, *US* 2627753, Espírito Santo, Brazil; *Rossetto* 445 (RB), Linhares, Espírito Santo, Brazil. *Leucaster caniflorus* (Mart.) Choisy, *US* 2839822, Jacarepaguá, Rio de Janeiro, Brazil; *Rossetto* 447 (RB), Linhares, Espírito Santo, Brazil; *Rossetto* 455 (RB), Teófilo Otoni, Minas Gerais, Brazil. *Ramisia brasiliensis* Oliv., *US* 2947296, Nova Venécia, Espírito Santo, Brazil; *Rossetto* 448 (RB), Nanuque, Minas Gerais, Brazil. *Reichenbachia hirsuta* Spreng., *Nee* 64109 (USZ), Living Collection Jardín Botánico Municipal de Santa Cruz de la Sierra, Santa Cruz de la Sierra, Bolivia; *Nee* 64169 (USZ), Rio Grande, Santa Cruz de la Sierra, Bolivia.

Outgroups

Agdestidaceae: *Agdestis clematidea* Moc. & Sessé ex DC., Carlquist, 1999. Petiveriaceae: *Gallesia integrifolia* (Spreng.) Harms, SPFW 5241; *Rossetto* 446 (RB), Linhares, Espírito Santo, Brazil; Carlquist, 2000; *Hillieria latifolia* (Lam.) H.Walter, Carlquist, 2000; *Monococcus echinophorus* F.Muell., Jansen et al., 2000; *Petiveria alliaceae* L., Carlquist, 2000; Duarte and Lopes, 2005; *Trichostigma octandrum* (L.) H.Walter, Carlquist, 2000; *Rivina humilis* L., Carlquist, 2000; Pugliali and Marquete, 1989; *Seguieria americana* L., *Rossetto* 451 (RB), Nanuque, Minas Gerais, Brazil; Carlquist, 2000; *Seguieria langsdorffii* Moq., *Rossetto* 452 (RB), Nanuque, Minas Gerais, Brazil. Phytolaccaceae: *Phytolacca dioica* L., Kirchoff and Fahn, 1984; Carlquist, 2000; *Phytolacca* sp., SPFW 5601.